

Stochastic modeling and analysis of Hepatitis and Tuberculosis co-infection dynamics

Sayed Murad Ali Shah, Yufeng Nie(聂玉峰), Anwarud Din, Abdulwasea Alkhazzan, and Bushra Younas

Citation: Chin. Phys. B, 2024, 33 (**11**): 110203. DOI: 10.1088/1674-1056/ad7afa
Journal homepage: http://cpb.iphy.ac.cn; http://iopscience.iop.org/cpb

What follows is a list of articles you may be interested in

Dynamic properties of rumor propagation model induced by Lévy noise on social networks

Ying Jing(景颖), Youguo Wang(王友国), Qiqing Zhai(翟其清), and Xianli Sun(孙先莉)
Chin. Phys. B, 2024, 33 (**9**): 090203. DOI: 10.1088/1674-1056/ad58c5

Sparse identification method of extracting hybrid energy harvesting system from observed data

Ya-Hui Sun(孙亚辉), Yuan-Hui Zeng(曾远辉), and Yong-Ge Yang(杨勇歌)
Chin. Phys. B, 2022, 31 (**12**): 120203. DOI: 10.1088/1674-1056/ac9cbf

Dynamical behavior and optimal impulse control analysis of a stochastic rumor spreading model

Liang'an Huo(霍良安) and Xiaomin Chen(陈晓敏)
Chin. Phys. B, 2022, 31 (**11**): 110204. DOI: 10.1088/1674-1056/ac98fb

Most probable transition paths in eutrophicated lake ecosystem under Gaussian white noise and periodic force

Jinlian Jiang(姜金连), Wei Xu(徐伟), Ping Han(韩平), and Lizhi Niu(牛立志)
Chin. Phys. B, 2022, 31 (**6**): 060203. DOI: 10.1088/1674-1056/ac5616

Exact solutions of stochastic fractional Korteweg de-Vries equation with conformable derivatives

Hossam A. Ghany, Abd-Allah Hyder, M Zakarya
Chin. Phys. B, 2020, 29 (**3**): 030203. DOI: 10.1088/1674-1056/ab75c9

Stochastic modeling and analysis of hepatitis and tuberculosis co-infection dynamics

Sayed Murad Ali Shah[1], Yufeng Nie(聂玉峰)[1,†], Anwarud Din[2,‡], Abdulwasea Alkhazzan[1], and Bushra Younas[3]

[1] *School of Mathematics and Statistics, Northwestern Polytechnical University, Xi'an* 710072, *China*
[2] *Department of Mathematics, Sun Yat-sen University, Guangzhou* 510275, *China*
[3] *Department of Mathematics, University of Sialkot, P. O. Box* 052, *Pakistan*

(Received 30 June 2024; revised manuscript received 27 August 2024; accepted manuscript online 14 September 2024)

Several mathematical models have been developed to investigate the dynamics of tuberculosis (TB) and hepatitis B virus (HBV). Numerous current models for TB, HBV, and their co-dynamics fall short in capturing the important and practical aspect of unpredictability. It is crucial to take into account a stochastic co-infection HBV–TB epidemic model since different random elements have a substantial impact on the overall dynamics of these diseases. We provide a novel stochastic co-model for TB and HBV in this study, and we establish criteria on the uniqueness and existence of a non-negative global solution. We also looked at the persistence of the infections as long its dynamics are governable by the proposed model. To verify the theoretical conclusions, numerical simulations are presented keeping in view the associated analytical results. The infections are found to finally die out and go extinct with certainty when Lévy intensities surpass the specified thresholds and the related stochastic thresholds fall below unity. The findings also demonstrate the impact of noise on the decline in the co-circulation of HBV and TB in a given population. Our results provide insights into effective intervention strategies, ultimately aiming to improve the management and control of TB and HBV co-infections.

Keywords: tuberculosis (TB), hepatitis B virus (HBV), white noise, Lévy noise, stochastic model

PACS: 02.50.Ey, 02.50.Fz, 02.50.Ga **DOI:** 10.1088/1674-1056/ad7afa

1. Introduction

Co-infection of tuberculosis (TB) and hepatitis B virus (HBV) is a major concern for global health challenge due to the high prevalence and public health impacts of both diseases, especially in regions with limited resources. This note explores the epidemiology, pathophysiology, clinical implications, and management strategies for TB and HBV coinfection. TB and HBV are both major global health issues. TB is ranked among the top 10 leading causes of mortality globally, as of World Health Organization (WHO). In 2018, the number of newly reported cases of TB was approximately 10 million, and the disease was responsible for causing 1.5 million deaths.[1] Similarly, HBV affects approximately 257 million people globally, leading to cirrhosis, hepatocellular carcinoma (HCC), and chronic liver disease.[2] Coinfection rates vary by region, with higher prevalence in areas where both diseases are endemic, such as Sub-Saharan Africa and parts of Asia. TB and HBV both impair the immune system but in different ways. TB primarily affects the lungs, although it can disseminate to other organs. It induces a strong cellular immune response which can exacerbate liver inflammation and damage in HBV-infected individuals. HBV, on the other hand, can cause chronic hepatitis, leading to liver cirrhosis and HCC. Co-infection complicates the clinical course of both diseases by altering immune responses and potentially accelerating disease progression.[3]

One of the effective methods for exploring the factors responsible for the spread of infectious diseases within a community is the techniques of mathematical modeling. It guides public health planning and responses against diverse infectious hazards in addition to aiding in the knowledge of transmission patterns and potential consequences for particular illnesses.[4–8] Furthermore, the mathematical modeling of infectious illnesses benefits more from the application of deterministic and fractional derivatives than from classical derivatives. Because fractional derivatives are better suited to represent the dynamics of memory effects, which are a common feature of biological processes, the resulting models are more realistic and accurate.[9–12] The mathematical models of infectious diseases transmission should also take into consideration the effect of random fluctuations in the dynamics of diseases, which can be investigated via stochastic models. These models are formulated depending on the underlying assumptions of the time and the state variables.[13–15] One type of these stochastic models is when the parameters of the models are perturbed via a Wiener process.[16–19] Some other models, such as those of liver cancer, also exist.[20,21] With one-dimensional white noise, it showed that this noise affected the extinction of the disease. This result was extended by Ji *et al.*[22] to show that when the endemic equilibrium exists then the small noise could lead to the persistence of the disease.

†Corresponding author. E-mail: yfnie@nwpu.edu.cn
‡Corresponding author. E-mail: anwarud@mail.sysu.edu.cn

© 2024 Chinese Physical Society and IOP Publishing Ltd

Co-epidemics of infectious diseases must be studied in order to better understand how diseases relate to one another and to develop preventative and treatment plans. In addition to providing useful insights into the intricate dynamics of the co-infections, mathematical models aid in the identification of efficient management strategies. The emerging scientists in their research addresses the dynamics of epidemics from various perspectives, whereas the majority of mathematical models concentrate on a single illness.[23,24] Nonetheless, there are not many instances of mathematical research on co-infection models in the literature.[25,26] Though co-infection models have received less attention, several important researches have advanced our knowledge of TB and HIV co-epidemics. While Bacaër *et al.*[27] predicted TB transmission in a South African township using numerical simulations, Naresh *et al.*[28] created a nonlinear model for TB/HIV co-infection. To account for treatment effects, Sharomi *et al.*[29] evaluated HIV/TB dynamics, whereas Roeger *et al.*[30] investigated co-infection using a model that allowed for simultaneous infections. These investigations highlight the usefulness of mathematical models in identifying and managing co-infections, although further study in this field is still required.

By determining the conditions under which the endemic and disease-free equilibrium points exhibit local or global asymptotic stabilities, one may forecast the persistence or elimination of a disease within a deterministic framework. The addition of stochastic noise, as we shall show, ruins these outcomes.[31–33] Moreover, in stochastic models, especially when affected by Gaussian or Lévy noise, the conditions that ensure the persistence or eradication of the diseases are no longer applicable purely from deterministic point of view.[34,35] We use stochastic modeling in order to provide a stronger basis for our study. By adding stochastic perturbations in the form of Lévy noise to each equation of the suggested deterministic model, we are able to overcome the drawbacks of deterministic models. To better represent the real-world events, we take into account independent jump processes for every sub-population in this setting. This method effectively reflects the variation in discrete elements that impact the dynamics among various sub-populations.

In this study, we are trying to consider some important epidemiological and biological features of both TB and HBV and formulate a stochastic mathematical model that is more realistic and easy to deal with. A thorough qualitative analysis of the model is the key contribution of the present work to the existing body of the literature. Our understanding is that this is the first comprehensive mathematical modeling for investigation of the qualitative dynamics of HBV–TB co-infection.

This paper is structured as follows: Section 2 presents the development of the model for TB and HBV co-infection. In Section 3, we discuss the global positivity of the solution for this co-infection model. Section 4 examines the conditions under which the model predicts extinction. Section 5 explores the persistence of the co-infection model. Numerical simulations that support our theoretical results are provided in Section 6. Section 7 gives a comprehensive summary of our work. Lastly, Section 8 contains our conclusion remarks.

2. Model formulation

At any time t, the total population $N(t)$ consists of the following epidemiological states: susceptible individuals (S) which can catch both the diseases at any time t, individuals infected with HBV (I_{H}), individuals infected with TB (I_{T}), individuals co-infected with TB and HBV (I_{HT}), and recovered individuals (R). The model incorporates the transmission rates of TB and HBV, natural mortality, treatment rates, and recovery rates. The susceptible population has the recruitment rate Ψ and these are via birth or coming into this population from the outside. All possible interactions of one disease with other are captured with the help of bilinear incidence rate. Further, the model assumes mortality and recovery rates in the associated compartments.

To create a new model for the co-infection of the TB and HBV, we make use of a compartmental approach to capture the dynamics

$$
\begin{aligned}
\frac{\mathrm{d}S(t)}{\mathrm{d}t} &= \Psi - \frac{\beta_{\mathrm{H}} I_{\mathrm{H}}(t) S(t)}{N} - \frac{\beta_{\mathrm{T}} I_{\mathrm{T}}(t) S(t)}{N} - \frac{\beta_{\mathrm{HT}} I_{\mathrm{HT}}(t) S(t)}{N} - dS(t),\\
\frac{\mathrm{d}I_{\mathrm{H}}(t)}{\mathrm{d}t} &= \frac{\beta_{\mathrm{H}} I_{\mathrm{H}}(t) S(t)}{N} - \frac{\delta_1 I_{\mathrm{H}}(t) I_{\mathrm{T}}(t)}{N} - (\alpha_1 + \alpha_2 + d) I_{\mathrm{H}}(t),\\
\frac{\mathrm{d}I_{\mathrm{T}}(t)}{\mathrm{d}t} &= \frac{\beta_{\mathrm{T}} I_{\mathrm{T}}(t) S(t)}{N} - \frac{\delta_2 I_{\mathrm{T}}(t) I_{\mathrm{H}}(t)}{N} - (\gamma_1 + \gamma_2 + d) I_{\mathrm{T}}(t),\\
\frac{\mathrm{d}I_{\mathrm{HT}}(t)}{\mathrm{d}t} &= \frac{\beta_{\mathrm{HT}} I_{\mathrm{HT}}(t) S(t)}{N} + \frac{\delta_1 I_{\mathrm{H}}(t) I_{\mathrm{T}}(t)}{N} + \frac{\delta_2 I_{\mathrm{T}}(t) I_{\mathrm{H}}(t)}{N} - (\eta_1 + \eta_2 + d) I_{\mathrm{HT}}(t),\\
\frac{\mathrm{d}R(t)}{\mathrm{d}t} &= \alpha_1 I_{\mathrm{H}}(t) + \gamma_1 I_{\mathrm{T}}(t) + \eta_1 I_{\mathrm{HT}}(t) - dR(t).
\end{aligned} \tag{1}
$$

Table 1. Parameters and their explanations.

Parameters	Explanation	Source
Ψ	rate of new susceptible individuals entering population	assumed
d	natural death rate	Ref. [36]
β_{T}	transmission rate of TB	Ref. [36]
β_{H}	transmission rate of HBV	Ref. [36]
β_{HT}	transmission rate of HBV and TB	Ref. [36]
α_1	recovery rate from HBV	assumed
α_2	death rate due to HBV	assumed
γ_1	TB recovery rate for individuals	assumed
γ_2	death rate due to TB	assumed
η_1	recovery rate from HBV and TB	Ref. [36]
η_2	death rate due to HBV and TB	Ref. [36]
δ_1	HBV and TB infection rate	assumed
δ_2	HBV and TB infection rate	assumed

The parameters in the model are well described in Table 1.

Constructing and analyzing this coinfection model represents a novel and essential step toward addressing the dual burden of TB and HBV. It provides a robust tool for researchers and public health officials to design and implement more effective control measures, ultimately contributing to better management and reduction of these coexisting infectious diseases.

(i) Disease-free equilibrium point

The disease-free equilibrium (DFE) of a mathematical model represents a state where the population has no presence of the disease, i.e., the number of infected individuals is zero. For the given model, we find the DFE by setting the rates of change of all compartments involving infected individuals to zero and solving for the equilibrium values. At the DFE, there are no infected individuals, so $I_{\mathrm{H}}=0$, $I_{\mathrm{T}}=0$, and $I_{\mathrm{HT}}=0$. Thus, we set $I_{\mathrm{H}}=0$, $I_{\mathrm{T}}=0$, and $I_{\mathrm{HT}}=0$ in the system of equations and solve for S and R

$$(S^*, I_{\mathrm{H}}^*, I_{\mathrm{T}}^*, I_{\mathrm{HT}}^*, R^*) = \left(\frac{\Psi}{d}, 0, 0, 0, 0\right). \tag{2}$$

(ii) Stability of the disease-free equilibrium

The stability of the DFE is crucial for predicting the potential for an epidemic. To evaluate this stability, we commonly examine the basic reproduction number (BRN), $\mathbb{R}_0^{\mathrm{D}}$. This number denotes the mean number of secondary infections produced by a single infected person in a population where everyone is vulnerable to the virus. When the BRN $\mathbb{R}_0^{\mathrm{D}}$ is less than 1, the DFE is stable, indicating that the infection is likely to be eradicated. Conversely, if $\mathbb{R}_0^{\mathrm{D}}$ exceeds 1, the DFE becomes unstable, suggesting that an epidemic could occur.

$$\mathbb{R}_0^{\mathrm{D}} = \mathrm{Max}\left(\frac{\beta_{\mathrm{H}}}{\alpha_1+\alpha_2+d}, \frac{\beta_{\mathrm{T}}}{\gamma_1+\gamma_2+d}, \frac{\beta_{\mathrm{HT}}}{\eta_1+\eta_2+d}\right). \tag{3}$$

This calculation shows that $\mathbb{R}_0^{\mathrm{D}}$ depends on the transmission rates of TB and HBV (β_{T}), (β_{H}), and (β_{HT}), and the combined rates of recovery, treatment, and natural death $(\alpha_1+\alpha_2+d), (\gamma_1+\gamma_2+d), (\eta_1+\eta_2+d)$. These factors collectively determine the potential for the spread of coinfection within the population.

The dynamical behavior of most epidemics, such as TB and HBV, is greatly influenced by random factors. By incorporating both white noise and Lévy noise into the model (1) co-infection model, we improve its ability to capture the complex, dynamic nature of infectious disease spread, ensuring more accurate predictions, and better informing public health strategies and interventions.

$$\begin{aligned}
\frac{\mathrm{d}S(t)}{\mathrm{d}t} &= \Psi - \frac{\beta_{\mathrm{H}} I_{\mathrm{H}}(t) S(t)}{N} - \frac{\beta_{\mathrm{T}} I_{\mathrm{T}}(t) S(t)}{N} - \frac{\beta_{\mathrm{HT}} I_{\mathrm{HT}}(t) S(t)}{N} - dS(t) + \sigma_1 S(t) dW_1(t) + \int_X Z_1(x) S(t^-) \tilde{N}(\mathrm{d}t, \mathrm{d}x),\\
\frac{\mathrm{d}I_{\mathrm{H}}(t)}{\mathrm{d}t} &= \frac{\beta_{\mathrm{H}} I_{\mathrm{H}}(t) S(t)}{N} - \frac{\delta_1 I_{\mathrm{H}}(t) I_{\mathrm{T}}(t)}{N} - (\alpha_1+\alpha_2+d) I_{\mathrm{H}}(t) + \sigma_2 I_{\mathrm{H}}(t) dW_2(t) + \int_X Z_2(x) I_{\mathrm{H}}(t^-) \tilde{N}(\mathrm{d}t, \mathrm{d}x),\\
\frac{\mathrm{d}I_{\mathrm{T}}(t)}{\mathrm{d}t} &= \frac{\beta_{\mathrm{T}} I_{\mathrm{T}}(t) S(t)}{N} - \frac{\delta_2 I_{\mathrm{T}}(t) I_{\mathrm{H}}(t)}{N} - (\gamma_1+\gamma_2+d) I_{\mathrm{T}}(t) + \sigma_3 I_{\mathrm{T}}(t) dW_3(t) + \int_X Z_3(x) I_{\mathrm{T}}(t^-) \tilde{N}(\mathrm{d}t, \mathrm{d}x),\\
\frac{\mathrm{d}I_{\mathrm{HT}}(t)}{\mathrm{d}t} &= \frac{\beta_{\mathrm{HT}} I_{\mathrm{HT}}(t) S(t)}{N} + \frac{\delta_1 I_{\mathrm{H}}(t) I_{\mathrm{T}}(t)}{N} + \frac{\delta_2 I_{\mathrm{T}}(t) I_{\mathrm{H}}(t)}{N} - (\eta_1+\eta_2+d) I_{\mathrm{HT}}(t) + \sigma_4 I_{\mathrm{HT}}(t) dW_4(t)\\
&\quad + \int_X Z_4(x) I_{\mathrm{HT}}(t^-) \tilde{N}(\mathrm{d}t, \mathrm{d}x),\\
\frac{\mathrm{d}R(t)}{\mathrm{d}t} &= \alpha_1 I_{\mathrm{H}}(t) + \gamma_1 I_{\mathrm{T}}(t) + \eta_1 I_{\mathrm{HT}}(t) - dR(t) + \sigma_5 R(t) dW_5(t) + \int_X Z_5(x) R(t^-) \tilde{N}(\mathrm{d}t, \mathrm{d}x),
\end{aligned} \tag{4}$$

where $dW_i(t)$, $(i=1,\ldots,5)$ represents independent Wiener processes (white noise) with mean zero and variance $\mathrm{d}t$, affecting each compartment $S, I_{\mathrm{H}}, I_{\mathrm{T}}, I_{\mathrm{HT}}, R$ with intensities σ_1, σ_2, σ_3, σ_4, and σ_5, respectively. Defined on a filtered probability triple (stochastic basis) $\left(\Omega, \mathcal{F}, (\mathcal{F}_t)_{t\geqslant 0}, \mathbb{P}\right)$ equipped with a filtration satisfying the usual criteria. $S(t^-)$, $I_{\mathrm{H}}(t^-)$, $I_{\mathrm{T}}(t^-)$, $R(t^-)$, $I_{\mathrm{TH}}(t^-)$ denote the left limits of $S(t)$, $I_{\mathrm{H}}(t)$, $I_{\mathrm{T}}(t)$, $R(t)$, $I_{\mathrm{TH}}(t)$. $\mathcal{Z}_n$ $(n=1,\ldots,5)$ are five independent Poisson countings associated with five finite characteristic Lévy measures $\tilde{N}_n$ $(L=1,\ldots,5)$ defined on a measurable set $\mathbb{R}^5\backslash\{0\}$.

3. Global existence and positivity

Certainly! Let us formulate a theorem and establish the global positivity of solutions for the stochastic epidemic model (4), which incorporates TB and HBV co-infection dynamics, white noise, and Lévy noise. Consider the stochastic TB and HBV co-infection model (4) described by the system of differential equations, where $S(t)$, $I_{\rm H}(t)$, $I_{\rm T}(t)$, $I_{\rm HT}(t)$, $R(t) \geq 0$, and $N(\mathrm{d}t, \mathrm{d}x)$ represents a Poisson random measure with intensity measure $\mathrm{d}x$.

Theorem 1 Given any starting points

$$\mathcal{X}_0 = (S(0), I_{\rm H}(0), I_{\rm T}(0), I_{\rm HT}(0), R(0)) \in \mathcal{D},$$

the perturbed system (4) has a unique global solution $\mathcal{X}_t = \mathcal{X}(t) = (S(t), I_{\rm H}(t), I_{\rm T}(t), I_{\rm HT}(t), R(t))$ for $t \geq 0$, which remains in $\mathcal{D}$ with unit probability, that is

$$\mathbb{P}\Big\{(S(t), I_{\rm H}(t), I_{\rm T}(t), I_{\rm HT}(t), R(t)) \in \mathcal{D}\ \forall\, t \geq 0\Big\} = 1.$$

Proof The coefficients of model (4) are 'locally Lipschitz continuous'. Given any initial states $\mathcal{X}_0 = (S(0), I_{\rm H}(0), I_{\rm T}(0), I_{\rm HT}(0), R(0)) \in \mathcal{D}$, there is a unique local solution $\mathcal{X}_t = \mathcal{X}(t) = (S(t), I_{\rm H}(t), I_{\rm T}(t), I_{\rm HT}(t), R(t))$ on $t \in [0, \tau_{\rm e})$, with $\tau_{\rm e}$ being the explosion time.[31] Suppose, $\rho_0 > 0$ is relatively large so that $S(0)$, $I_{\rm H}(0)$, $I_{\rm T}(0)$, $I_{\rm HT}(0)$, $R(0)$ all exist in $[1/\rho_0, \rho_0]$. Now, $\forall \rho \geq \rho_0$, let us define

$$\tau_\rho = \inf\left\{t \in [0, \tau_{\rm e}) : S(t) \notin \left(\frac{1}{\rho}, \rho\right) \text{ or } I_{\rm H}(t) \notin \left(\frac{1}{\rho}, \rho\right) \text{ or } I_{\rm T}(t) \notin \left(\frac{1}{\rho}, \rho\right) \text{ or } I_{\rm HT}(t) \notin \left(\frac{1}{\rho}, \rho\right) \text{ or } R(t) \notin \left(\frac{1}{\rho}, \rho\right)\right\}, \quad (5)$$

where, $\inf \phi = \infty$, and ϕ represents the empty set. It is clear that, τ_ρ is increasing as $\rho \to \infty$. We have $\tau_\infty = \lim_{\rho\to\infty} \tau_\rho$, so that $\tau_\infty \leq \tau_{\rm e}$ almost surely (a.s.). We only need to show $\tau_\infty = \infty$ a.s., so that $\tau_{\rm e} = \infty$ and $(S(t), I_{\rm H}(t), I_{\rm T}(t), I_{\rm HT}(t), R(t)) \in \mathcal{D}$ a.s for all $t \geq 0$.

Suppose $\tau_\infty < \infty$, then we shall have a pair of constants $T > 0$ and $\zeta \in (0,1)$ such that $\mathbb{P}\{t_{\infty \leq T}\} > \zeta$, so that we have an integer $\rho_1 \geq \rho_0$ with

$$\mathbb{P}\{t_{\infty \leq T}\} \geq \zeta\ \forall\, \rho \geq \rho_1. \quad (6)$$

Define $\mathcal{C}^2$ function $\mathcal{V}_1 : \mathbb{R}^5_+ \to \mathbb{R}_+$ by

$$\mathcal{V}_1(S, I_{\rm H}, I_{\rm T}, I_{\rm HT}, R) = (S - 1 - \ln S) + (I_{\rm H} - 1 - \ln I_{\rm H}) + (I_{\rm T} - 1 - \ln I_{\rm T}) + (I_{\rm HT} - 1 - \ln I_{\rm HT}) + (R - 1 - \ln R). \quad (7)$$

Applying Itô's formula on Eq. (7), we have

$$\begin{aligned} d\mathcal{V}_1(S, I_{\rm H}, I_{\rm T}, I_{\rm HT}, R) = {} & L\mathcal{V}_1\, \mathrm{d}t + \sigma_1(S-1)\, dW_1(t) + \sigma_2(I_{\rm H}-1)\, dW_2(t) + \sigma_3(I_{\rm T}-1)\, dW_3(t) \\ & + \sigma_4(I_{\rm HT}-1)\, dW_4(t) + \sigma_5(R-1)\, dW_5(t) + \int_X [Z_1(x)S - \ln(1+Z_1(x))]\tilde{N}(\mathrm{d}t, \mathrm{d}x) \\ & + \int_X [Z_2(x)I_{\rm H} - \ln(1+Z_2(x))]\tilde{N}(\mathrm{d}t, \mathrm{d}x) + \int_X [Z_3(x)I_{\rm T} - \ln(1+Z_3(x))]\tilde{N}(\mathrm{d}t, \mathrm{d}x) \\ & + \int_X [Z_4(x)I_{\rm HT} - \ln(1+Z_4(x))]\tilde{N}(\mathrm{d}t, \mathrm{d}x) + \int_X [Z_5(x)R - \ln(1+Z_5(x))]\tilde{N}(\mathrm{d}t, \mathrm{d}x), \end{aligned} \quad (8)$$

where

$$\begin{aligned} d\mathcal{V}_1 = {} & \left(1 - \frac{1}{S}\right)\left(\Psi - \frac{\beta_{\rm H} I_{\rm H} S}{N} - \frac{\beta_{\rm T} I_{\rm T} S}{N} - \frac{\beta_{\rm HT} I_{\rm HT} S}{N} - dS\right)\mathrm{d}t + \frac{\sigma_1^2}{2} + \int_X [Z_1(x) - \ln(1+Z_1(x))]\nu \mathrm{d}x \\ & + \left(1 - \frac{1}{I_{\rm H}}\right)\left(\frac{\beta_{\rm H} I_{\rm H} S}{N} - \frac{\delta_1 I_{\rm H} I_{\rm T}}{N} - (\alpha_1 + \alpha_2 + d) I_{\rm H}\right)\mathrm{d}t + \frac{\sigma_2^2}{2} + \int_X [Z_2(x) - \ln(1+Z_2(x))]\nu \mathrm{d}x \\ & + \left(1 - \frac{1}{I_{\rm T}}\right)\left(\frac{\beta_{\rm T} I_{\rm T} S}{N} - \frac{\delta_2 I_{\rm T} I_{\rm H}}{N} - (\gamma_1 + \gamma_2 + d) I_{\rm T}\right)\mathrm{d}t + \frac{\sigma_3^2}{2} + \int_X [Z_3(x) - \ln(1+Z_3(x))]\nu \mathrm{d}x \\ & + \left(1 - \frac{1}{I_{\rm HT}}\right)\left(\frac{\beta_{\rm HT} I_{\rm HT} S}{N} + \frac{\delta_1 I_{\rm H} I_{\rm T}}{N} + \frac{\delta_2 I_{\rm T} I_{\rm H}}{N} - (\eta_1 + \eta_2 + d) I_{\rm HT}\right)\mathrm{d}t \\ & + \frac{\sigma_4^2}{2} + \int_X [Z_4(x) - \ln(1+Z_4(x))]\nu \mathrm{d}x \\ & + \left(1 - \frac{1}{R}\right)\left(\alpha_1 I_{\rm H} + \alpha_1 I_{\rm H} + \gamma_1 I_{\rm T} + \eta_1 I_{\rm HT} - dR\right)\mathrm{d}t + \frac{\sigma_5^2}{2} + \int_X [Z_5(x) - \ln(1+Z_5(x))]\nu \mathrm{d}x, \\ \mathcal{L}\mathcal{V}_1 = {} & (\Psi - dS - dI_{\rm H} - dI_{\rm T} - dI_{\rm HT} - dR) + \left[-\frac{\Psi}{S} + \frac{\beta_{\rm H} I_{\rm H}}{N} + \frac{\beta_{\rm T} I_{\rm T}}{N} + \frac{\beta_{\rm HT} I_{\rm HT}}{N} + d\right] \\ & + \left[-\frac{\beta_{\rm H} S}{N} + \frac{\delta_1 I_{\rm T}}{N} + (\alpha_1 + \alpha_2 + d) - \frac{\beta_{\rm T} S}{N} + \frac{\delta_2 I_{\rm H}}{N} + (\gamma_1 + \gamma_2 + d) - \frac{\beta_{\rm HT} S}{N} - \frac{\delta_1 I_{\rm H} I_{\rm T}}{I_{\rm HT} N} - \frac{\delta_2 I_{\rm T} I_{\rm H}}{I_{\rm HT} N}\right. \end{aligned}$$

$$
\begin{aligned}
&+(\eta_1+\eta_2+d)\Big]+\Big[-\frac{\alpha_1 I_{\rm H}}{R}-\frac{\gamma_1 I_{\rm T}}{R}-\frac{\eta_1 I_{\rm HT}}{R}+d\Big]+\frac{1}{2}\sigma_1^2+\frac{1}{2}\sigma_2^2+\frac{1}{2}\sigma_3^2+\frac{1}{2}\sigma_4^2+\frac{1}{2}\sigma_5^2\\
&+\int_X[Z_1(x)-\ln(1-Z_1(x))]\nu\,{\rm d}x+\int_X[Z_2(x)-\ln(1-Z_2(x))]\nu\,{\rm d}x+\int_X[Z_3(x)-\ln(1-Z_3(x))]\nu\,{\rm d}x\\
&+\int_X[Z_4(x)-\ln(1-Z_4(x))]\nu\,{\rm d}x+\int_X[Z_5(x)-\ln(1-Z_5(x))]\nu\,{\rm d}x,\\
\mathcal{L}\mathcal{V}_1 \le\ &\Psi-dN+(\alpha_1+\alpha_2+d)+(\gamma_1+\gamma_2+d)+(\eta_1+\eta_2+d)\\
&+d+\frac{\beta_{\rm H}I_{\rm H}}{N}+\frac{\beta_{\rm T}I_{\rm T}}{N}+\frac{\beta_{\rm HT}I_{\rm HT}}{N}+\frac{\delta_1 I_{\rm T}}{N}+\frac{\delta_2 I_{\rm H}}{N}\\
&+\frac{1}{2}\sigma_1^2+\frac{1}{2}\sigma_2^2+\frac{1}{2}\sigma_3^2+\frac{1}{2}\sigma_4^2+\frac{1}{2}\sigma_5^2+\int_X[Z_1(x)-\ln(1-Z_1(x))]\nu\,{\rm d}x+\int_X[Z_2(x)-\ln(1-Z_2(x))]\nu\,{\rm d}x\\
&+\int_X[Z_3(x)-\ln(1-Z_3(x))]\nu\,{\rm d}x+\int_X[Z_4(x)-\ln(1-Z_4(x))]\nu\,{\rm d}x+\int_X[Z_5(x)-\ln(1-Z_5(x))]\nu\,{\rm d}x. \qquad (9)
\end{aligned}
$$

Noting that $S+I_{\rm H}+I_{\rm T}+I_{\rm HT}+R\le\Psi/d$, $I_{\rm H}/N\le 1$, $I_{\rm T}/N\le 1$, we have

$$
\begin{aligned}
\mathcal{L}\mathcal{V}_1 \le\ &5d+\alpha_1+\alpha_2+\gamma_1+\gamma_2+\eta_1+\eta_2+\beta_{\rm H}+\beta_{\rm T}+\beta_{\rm HT}+\delta_1+\delta_2+\frac{1}{2}\sigma_1^2+\frac{1}{2}\sigma_2^2\\
&+\frac{1}{2}\sigma_3^2+\frac{1}{2}\sigma_4^2+\frac{1}{2}\sigma_5^2+G^*=:G, \qquad (10)
\end{aligned}
$$

where $G^*=\max\{\int_X[Z_i(x)-\ln(1+Z_i(x))]\tilde{N}({\rm d}t,{\rm d}x)\}$, $i=\{1,2,3,4,5\}$.

Since G is a positive constant which is independent of S, $I_{\rm H}$, $I_{\rm T}$, $I_{\rm HT}$, R, and t, we can obtain

$$
\begin{aligned}
d\mathcal{V}_1(S,I_{\rm H},I_{\rm T},I_{\rm HT},R) \le\ &G\,{\rm d}t+\sigma_1(S-1)\,dW_1(t)+\sigma_2(I_{\rm H}-1)\,dW_2(t)+\sigma_3(I_{\rm T}-1)\,dW_3(t)\\
&+\sigma_4(I_{\rm HT}-1)\,dW_4(t)+\sigma_5(R-1)\,dW_5(t). \qquad (11)
\end{aligned}
$$

By integrating both sides of Eq. (11) from 0 to $T\wedge\tau_g$ and assuming expectations, we may get the following result

$$
\mathbb{E}[\mathcal{V}_1(S(T\wedge\tau_g),I_{\rm H}(T\wedge\tau_g),I_{\rm T}(T\wedge\tau_g),I_{\rm HT}(T\wedge\tau_g),R(T\wedge\tau_g))]\le\mathcal{V}_1(S(0),I_{\rm H}(0),I_{\rm T}(0),I_{\rm HT}(0),R(0))+GT<\infty. \qquad (12)
$$

Set $\Pi_g=\{\tau_g\le t\}$ for $g\ge g_1$ by Eq. (6), $P(\Pi_g)\ge\rho$. Noticing that for every $\pi\in\Pi_g$, there is at least one of $S(\tau_g,\pi)$, $I_{\rm H}(\tau_g,\pi)$, $I_{\rm T}(\tau_g,\pi)$, $I_{\rm HT}(\tau_g,\pi)$, and $R(\tau_g,\pi)$ that equals either g or $1/g$. Hence $S(\tau_g,\pi)$, $I_{\rm H}(\tau_g,\pi)$, $I_{\rm T}(\tau_g,\pi)$, $I_{\rm HT}(\tau_g,\pi)$, $R(\tau_g,\pi)$ are no less than $g-1-\ln g$ or $1/g-1-\ln 1/g=1/g-1+\ln g$. Consequently,

$$
\mathcal{V}_1(S(\tau_g,\pi),I_{\rm H}(\tau_g,\pi),I_{\rm T}(\tau_g,\pi),I_{\rm HT}(\tau_g,\pi),R(\tau_g,\pi))\ge(g-1-\ln g)\wedge\left(\frac{1}{g}-1+\ln g\right). \qquad (13)
$$

Here, $a\wedge b$ represents the minimum value between a and b. Considering Eqs. (12) and (13), it follows that

$$
\begin{aligned}
\mathcal{V}_1(S(0),I_{\rm H}(0),I_{\rm T}(0),I_{\rm HT}(0),R(0))+GT &\ge\mathbb{E}[I_{\Pi_g}\mathcal{V}_1(S(\tau_g,\pi),I_{\rm H}(\tau_g,\pi),I_{\rm T}(\tau_g,\pi),I_{\rm HT}(\tau_g,\pi),R(\tau_g,\pi))]\\
&\ge\varepsilon\left[(g-1-\ln g)\wedge\left(\frac{1}{g}-1+\ln g\right)\right], \qquad (14)
\end{aligned}
$$

where I_{Π_g} denotes the indicator function of Π_g. Allowing k to approach infinity results in a contradiction.

$$
\infty>\mathcal{V}_1(S(0),I_{\rm H}(0),I_{\rm T}(0),I_{\rm HT}(0),R(0))+GT=\infty.
$$

Hence, it follows that $\tau_\infty=\infty$ almost surely. This concludes the proof of Theorem 1.

4. Extinction analysis of the model

It is essential to investigate conditions under which an epidemic can be eliminated from the population while researching the dynamics of an epidemic system. We will talk about such situations in this part of the manuscript. First, some basic notations will be introduced, after which adequate conditions for the extinction of both illnesses will be derived. Let us suppose

$$
\langle X(t)\rangle=\frac{1}{t}\int_0^t X(s)\,{\rm d}s.
$$

Lemma 1 Let $(S,I_{\rm H},I_{\rm T},I_{\rm HT},R)$ be a solution of Eq. (4) subject to the conditions $(S(0),I_{\rm H}(0),I_{\rm T}(0),I_{\rm HT}(0),R(0))\in R_+^5$, then a.s.,

$$
\lim_{t\to\infty}\frac{S(t)+I_{\rm H}(t)+I_{\rm T}(t)+I_{\rm HT}(t)+R(t)}{t}=0. \qquad (15)
$$

Moreover, if $d > [(\sigma_1^2 \vee \sigma_2^2 \vee \sigma_3^2 \vee \sigma_4^2 \vee \sigma_5^2)]/2$, then

$$\begin{aligned}
&\lim_{t\to\infty}\frac{1}{t}\int_0^t S(u)\,\mathrm{d}W_1(u)=0,\\
&\lim_{t\to\infty}\frac{1}{t}\int_0^t I_{\mathrm{H}}(u)\,\mathrm{d}W_2(u)=0,\\
&\lim_{t\to\infty}\frac{1}{t}\int_0^t I_{\mathrm{T}}(u)\,\mathrm{d}W_3(u)=0,\\
&\lim_{t\to\infty}\frac{1}{t}\int_0^t I_{\mathrm{HT}}(u)\,\mathrm{d}W_4(u)=0,\\
&\lim_{t\to\infty}\frac{1}{t}\int_0^t R(u)\,\mathrm{d}W_5(u)=0. \qquad (16)
\end{aligned}$$

Since the findings may be obtained by applying the same strategy as in the proofs of Lemmas (2.1) and (2.2) from the work of Ref. [31], the proof of this lemma is not needed.

The stochastic system (4) threshold quantity $\mathbb{R}_0^{\mathrm{E}}$ may be written as follows:

$$\mathbb{R}_0^{\mathrm{E}} = \max\{\mathbb{R}_{\mathrm{H}}, \mathbb{R}_{\mathrm{T}}, \mathbb{R}_{\mathrm{HT}}\}, \qquad (17)$$

where

$$\begin{aligned}
\mathbb{R}_{\mathrm{H}} &= \frac{\beta_{\mathrm{H}}}{(\delta_1+\alpha_1+\alpha_2+d+\sigma_2^2/2+\int_X [Z_2(x)-\ln(1+Z_2(x))]v(\mathrm{d}x))},\\
\mathbb{R}_{\mathrm{T}} &= \frac{\beta_{\mathrm{T}}}{(\delta_2+\gamma_1+\gamma_2+d+\sigma_3^2/2+\int_X [Z_3(x)-\ln(1+Z_3(x))]v(\mathrm{d}x))},\\
\mathbb{R}_{\mathrm{HT}} &= \frac{\beta_{\mathrm{HT}}}{(\eta_1+\eta_2+d+\sigma_4^2/2+\int_X [Z_4(x)-\ln(1+Z_4(x))]v(\mathrm{d}x))}.
\end{aligned}$$

The following theorem is worthy to state for the extinction of infection.

Theorem 2 For any given initial value: $(S(0), I_{\mathrm{H}}(0), I_{\mathrm{T}}(0), I_{\mathrm{HT}}(0), R(0)) \in R^5$, the solution $(S(t), I_{\mathrm{H}}(t), I_{\mathrm{T}}(t), I_{\mathrm{HT}}(0)(t)R(t))$ of the system (4) has the following properties.

(i) If $\mathbb{R}_{\mathrm{H}} < 1$, then HBV goes to extinction almost surely (a.s). (ii) If $\mathbb{R}_{\mathrm{T}} < 1$, then goes to extinction a.s. (iii) If $\mathbb{R}_{\mathrm{HT}} < 1$, then the co-infection of both diseases goes into extinction a.s.

It means, if $d > [(\sigma_1^2 \vee \sigma_2^2 \vee \sigma_3^2 \vee \sigma_4^2 \vee \sigma_5^2)]/2$ and $\mathbb{R}_0^{\mathrm{E}} < 1$, then

$$\lim_{t\to\infty}\frac{\langle \ln I_{\mathrm{H}}(t)\rangle}{t} < 0, \quad \lim_{t\to\infty}\frac{\langle \ln I_{\mathrm{T}}(t)\rangle}{t} < 0, \quad \lim_{t\to\infty}\frac{\langle \ln I_{\mathrm{HT}}(t)\rangle}{t} < 0, \ \text{a.s.}$$

That is the diseases go into extinction with probability 1.

Moreover,

$$\lim_{t\to\infty}\langle S(t)\rangle = \frac{\Psi}{d}, \ \lim_{t\to\infty}\langle I_{\mathrm{H}}(t)\rangle = 0, \ \lim_{t\to\infty}\langle I_{\mathrm{T}}(t)\rangle = 0, \ \lim_{t\to\infty}\langle I_{\mathrm{HT}}(t)\rangle = 0, \ \lim_{t\to\infty}\langle R(t)\rangle = 0. \qquad (18)$$

Proof Integrating both sides from 0 to t for model (4), yields

$$\begin{aligned}
\frac{S(t)-S(0)}{t} &= \Psi - \frac{\beta_{\mathrm{H}}\langle I_{\mathrm{H}}S\rangle}{\langle N\rangle} - \frac{\beta_{\mathrm{T}}\langle I_{\mathrm{T}}S\rangle}{\langle N\rangle} - \frac{\beta_{\mathrm{HC}}\langle SI_{\mathrm{HT}}\rangle}{\langle N\rangle} - d\langle S\rangle + \frac{\sigma_1}{t}\int_0^t S(r)\,\mathrm{d}W_1(r)\\
&\quad + \frac{1}{t}\int_0^t\left[\int_X Z_1(x)S(t^-)\tilde{N}(\mathrm{d}t,\mathrm{d}x)\right]\mathrm{d}r,\\
\frac{I_{\mathrm{H}}(t)-I_{\mathrm{H}}(0)}{t} &= \frac{\beta_{\mathrm{H}}\langle I_{\mathrm{H}}S\rangle}{\langle N\rangle} - \frac{\delta_1\langle I_{\mathrm{H}}I_{\mathrm{T}}\rangle}{\langle N\rangle} - (\alpha_1+\alpha_2+d)\langle I_{\mathrm{H}}\rangle + \frac{\sigma_2}{t}\int_0^t S(r)\,\mathrm{d}W_2(r)\\
&\quad + \frac{1}{t}\int_0^t\left[\int_X Z_2(x)I_{\mathrm{H}}(t^-)\tilde{N}(\mathrm{d}t,\mathrm{d}x)\right]\mathrm{d}r,\\
\frac{I_{\mathrm{T}}(t)-I_{\mathrm{T}}(0)}{t} &= \frac{\beta_{\mathrm{T}}\langle I_{\mathrm{T}}S\rangle}{\langle N\rangle} - \frac{\delta_2\langle I_{\mathrm{T}}I_{\mathrm{H}}\rangle}{\langle N\rangle} - (\gamma_1+\gamma_2+d)\langle I_{\mathrm{T}}\rangle + \frac{\sigma_3}{t}\int_0^t I_{\mathrm{T}}(r)\,\mathrm{d}W_3(r)\\
&\quad + \frac{1}{t}\int_0^t\left[\int_X Z_3(x)I_{\mathrm{T}}(t^-)\tilde{N}(\mathrm{d}t,\mathrm{d}x)\right]\mathrm{d}r,\\
\frac{I_{\mathrm{HT}}(t)-I_{\mathrm{HT}}(0)}{t} &= \frac{\beta_{\mathrm{HT}}\langle I_{\mathrm{HT}}S\rangle}{\langle N\rangle} + \frac{\delta_1\langle I_{\mathrm{H}}I_{\mathrm{T}}\rangle}{\langle N\rangle} + \frac{\delta_2\langle I_{\mathrm{T}}I_{\mathrm{H}}\rangle}{\langle N\rangle} - (\eta_1+\eta_2+d)\langle I_{\mathrm{HT}}\rangle + \frac{\sigma_4}{t}\int_0^t I_{\mathrm{HT}}(r)\,\mathrm{d}W_4(r)\\
&\quad + \frac{1}{t}\int_0^t\left[\int_X Z_4(x)I_{\mathrm{HT}}(t^-)\tilde{N}(\mathrm{d}t,\mathrm{d}x)\right]\mathrm{d}r,
\end{aligned}$$

$$\frac{R(t)-R(0)}{t} = \alpha_1\langle I_{\rm H}\rangle + \gamma_1\langle I_{\rm T}\rangle + \eta_1\langle I_{\rm HT}\rangle - d\langle R(t)\rangle + \frac{\sigma_5}{t}\int_0^t R(r)\,{\rm d}W_5(r) + \frac{1}{t}\int_0^t\left[\int_X Z_5(x)R(t^-)\tilde{N}({\rm d}t,{\rm d}x)\right]{\rm d}r. \tag{19}$$

Proof (I) If we apply Itô formula to the second equation in Eq. (4), we have

$$d\ln I_{\rm H}(t) = \left[\frac{\beta_{\rm H}I_{\rm H}S}{N} - \frac{\delta_1 I_{\rm H}I_{\rm T}}{N} - (\alpha_1+\alpha_2+d)I_{\rm H}\right]\frac{1}{I_{\rm H}}{\rm d}t - \frac{\sigma_2^2}{2}{\rm d}t + \sigma_2\,{\rm d}W_2(t) - \int_X[Z_2(x)-\ln(1+Z_2(x))]v{\rm d}x. \tag{20}$$

If we integrate Eq. (20) within $[0,t]$ and then divide through by t, we have

$$\begin{aligned}\frac{\ln I_{\rm H}(t)-\ln I_{\rm H}(0)}{t} &= \beta_{\rm H}\frac{\langle S\rangle}{\langle N\rangle} - \delta_1\frac{\langle I_T\rangle}{\langle N\rangle} - (\alpha_1+\alpha_2+d) - \frac{\sigma_2^2}{2} + \frac{\sigma_2}{t}\int_0^t {\rm d}W_2(r)\\ &\quad + \frac{1}{t}\int_X[\ln(1+Z_2(x))]\tilde{N}({\rm d}t,{\rm d}x) - \int_X[Z_2(x)-\ln(1+Z_2(x))]v({\rm d}x)\\ &\le \beta_{\rm H} - (\delta_1+\alpha_1+\alpha_2+d) - \frac{\sigma_2^2}{2} + \frac{\sigma_2}{t}\int_0^t {\rm d}W_2(r)\\ &\quad + \frac{1}{t}\int_X[\ln(1+Z_2(x))]\tilde{N}({\rm d}t,{\rm d}x) - \int_X[Z_2(x)-\ln(1+Z_2(x))]v({\rm d}x)\\ &= \beta_{\rm H} - \left(\delta_1+\alpha_1+\alpha_2+d+\frac{\sigma_2^2}{2}+\int_X[Z_2(x)-\ln(1+Z_2(x))]v({\rm d}x)\right)\\ &\quad + \frac{\sigma_2}{t}\int_0^t {\rm d}W_2(r) + \frac{1}{t}\int_X[\ln(1+Z_2(x))]\tilde{N}({\rm d}t,{\rm d}x)\\ &= \left(\delta_1+\alpha_1+\alpha_2+d+\frac{\sigma_2^2}{2}+\int_X[Z_2(x)-\ln(1+Z_2(x))]v({\rm d}x)\right)(\boldsymbol{R}_{\rm H}-1)\\ &\quad + \frac{\sigma_2}{t}\int_0^t {\rm d}W_2(r) + \frac{1}{t}\int_X[\ln(1+Z_2(x))]\tilde{N}({\rm d}t,{\rm d}x).\end{aligned} \tag{21}$$

In addition, let

$$M_{\rm H}(t) = \frac{\sigma_2}{t}\int_0^t {\rm d}W_2(r) + \frac{1}{t}\int_X[\ln(1+Z_2(x))]\tilde{N}({\rm d}t,{\rm d}x),$$

be a continuous (locally) martingale and $M_{\rm H}(0)=0$. From Lemma 1 and $t\to\infty$, we have

$$\lim_{t\to\infty}\sup\frac{M_{\rm H}(t)}{t} = 0. \tag{22}$$

If $\mathbb{R}_{\rm H}<1$, then equation (21) becomes

$$\lim_{t\to\infty}\sup\frac{\ln I_{\rm H}(t)}{t} \le \left(\delta_1+\alpha_1+\alpha_2+d+\frac{\sigma_2^2}{2}+\int_X[Z_2(x)-\ln(1+Z_2(x))]v({\rm d}x)\right)\left(\mathbb{R}_{\rm H}-1\right) < 0, \quad \text{a.s.} \tag{23}$$

Equation (23) above implies

$$\lim_{t\to\infty} I_{\rm H}(t) = 0, \quad \text{a.s.} \tag{24}$$

Proof (II) Likewise, if Itô formula is applied to the third equation of Eq. (4), we have

$$\frac{\ln I_{\rm T}(t)-\ln I_{\rm T}(0)}{t} \le (\delta_2+\gamma_1+\gamma_2+d+\frac{\sigma_3^2}{2}+\int_X[Z_3(x)-\ln(1+Z_3(x))]v({\rm d}x))(\mathbb{R}_{\rm T}-1) + \frac{\sigma_3}{t}\int_0^t {\rm d}W_3(r) + \frac{1}{t}\int_X[\ln(1+Z_3(x))]\tilde{N}({\rm d}t,{\rm d}x). \tag{25}$$

Here let

$$M_{\rm T}(t) = \frac{\sigma_3}{t}\int_0^t {\rm d}W_3(r) + \frac{1}{t}\int_X[\ln(1+Z_3(x))]\tilde{N}({\rm d}t,{\rm d}x),$$

be a locally continuous martingale and $M_{\rm T}(0)=0$. With Lemma 1 and $t\to\infty$, we have

$$\lim_{t\to\infty}\sup\frac{M_{\rm T}(t)}{t} = 0. \tag{26}$$

If $\mathbb{R}_{\mathrm{T}} < 1$, then equation (25) results in

$$\limsup_{t\to\infty}\frac{\ln I_{\mathrm{T}}(t)}{t} \le \left(\delta_2+\gamma_1+\gamma_2+d+\frac{\sigma_3^2}{2}+\int_X[Z_3(x)-\ln(1+Z_3(x))]v(\mathrm{d}x)\right)\left(\mathbb{R}_{\mathrm{T}}-1\right) < 0, \quad \text{a.s.} \tag{27}$$

Equation (27) above implies

$$\lim_{t\to\infty} I_{\mathrm{T}}(t) = 0, \quad \text{a.s.} \tag{28}$$

Proof (III) Using Eq. (24), Eq. (28), and adopting Itô formula on the fourth equation of Eq. (4), we have

$$\begin{aligned}\frac{\ln I_{\mathrm{HT}}(t)-\ln I_{\mathrm{HT}}(0)}{t} \le{}& \left(\eta_1+\eta_2+d+\frac{\sigma_4^2}{2}+\int_X[Z_4(x)-\ln(1+Z_4(x))]v(\mathrm{d}x)\right)(\mathbb{R}_{\mathrm{HT}}-1)\\ &+\frac{\sigma_4}{t}\int_0^t \mathrm{d}W_4(r)+\frac{1}{t}\int_X[\ln(1+Z_4(x))]\tilde{N}(\mathrm{d}t,\mathrm{d}x).\end{aligned} \tag{29}$$

Let

$$M_{\mathrm{HT}}(t) = \frac{\sigma_4}{t}\int_0^t \mathrm{d}W_4(r)+\frac{1}{t}\int_X[\ln(1+Z_4(x))]\tilde{N}(\mathrm{d}t,\mathrm{d}x)$$

be a locally continuous martingale and $M_{\mathrm{HT}}(0)=0$. With Lemma 1 and $t\to\infty$, we obtain

$$\limsup_{t\to\infty}\frac{M_{\mathrm{HT}}(t)}{t} = 0. \tag{30}$$

If $\mathbb{R}_{\mathrm{HT}} < 1$ is satisfied, then equation (29) becomes

$$\limsup_{t\to\infty}\frac{\ln I_{\mathrm{HT}}(t)}{t} \le \left(\eta_1+\eta_2+d+\frac{\sigma_4^2}{2}+\int_X[Z_4(x)-\ln(1+Z_4(x))]v(\mathrm{d}x)\right)\left(\mathbb{R}_{\mathrm{HT}}-1\right) < 0 \ \text{ a.s.} \tag{31}$$

The above equation (31) implies that

$$\lim_{t\to\infty} I_{\mathrm{HT}}(t) = 0, \quad \text{a.s.} \tag{32}$$

The last equation of system (19), and using Eq. (24), Eq. (28), Eq. (32), and $t\to\infty$, then we can obtain

$$\lim_{t\to\infty}\langle R(t)\rangle = 0, \quad \text{a.s.}$$

From Eq. (19), yielding

$$\begin{aligned}&\frac{S(t)-S(0)}{t}+\frac{I_{\mathrm{H}}(t)-I_{\mathrm{H}}(0)}{t}+\frac{I_{\mathrm{T}}(t)-I_{\mathrm{T}}(0)}{t}+\frac{I_{\mathrm{HT}}(t)-I_{\mathrm{HT}}(0)}{t}\\
&=\Psi-\frac{\beta_{\mathrm{H}}\langle I_{\mathrm{H}}S\rangle}{\langle N\rangle}-\frac{\beta_{\mathrm{T}}\langle I_{\mathrm{T}}S\rangle}{\langle N\rangle}-\frac{\beta_{\mathrm{HT}}\langle SI_{\mathrm{HT}}\rangle}{\langle N\rangle}-d\langle S\rangle\frac{\beta_{\mathrm{H}}\langle I_{\mathrm{H}}S\rangle}{\langle N\rangle}-\frac{\delta_1\langle I_{\mathrm{H}}I_{\mathrm{T}}\rangle}{\langle N\rangle}-(\alpha_1+\alpha_2+d)\langle I_{\mathrm{H}}\rangle\\
&+\frac{\beta_{\mathrm{T}}\langle I_{\mathrm{T}}S\rangle}{\langle N\rangle}-\frac{\delta_2\langle I_{\mathrm{T}}I_{\mathrm{H}}\rangle}{\langle N\rangle}-(\gamma_1+\gamma_2+d)\langle I_{\mathrm{T}}\rangle+\frac{\beta_{\mathrm{HT}}\langle I_{\mathrm{HT}}S\rangle}{\langle N\rangle}+\frac{\delta_1\langle I_{\mathrm{H}}I_{\mathrm{T}}\rangle}{\langle N\rangle}+\frac{\delta_2\langle I_{\mathrm{T}}I_{\mathrm{H}}\rangle}{\langle N\rangle}-(\eta_1+\eta_2+d)\langle I_{\mathrm{HT}}\rangle\\
&+\frac{\sigma_1}{t}\int_0^t S(r)\mathrm{d}W_1(r)+\frac{\sigma_2}{t}\int_0^t I_{\mathrm{H}}\mathrm{d}W_2(r)+\frac{\sigma_3}{t}\int_0^t I_{\mathrm{T}}\mathrm{d}W_3(r)+\frac{\sigma_4}{t}\int_0^t I_{\mathrm{HT}}\mathrm{d}W_4(r)\\
&+\frac{1}{t}\int_0^t\left[\int_X Z_1(x)S(t^-)\tilde{N}(\mathrm{d}t,\mathrm{d}x)\right]\mathrm{d}r\\
&+\frac{1}{t}\int_0^t\left[\int_X Z_2(x)I_{\mathrm{H}}(t^-)\tilde{N}(\mathrm{d}t,\mathrm{d}x)\right]\mathrm{d}r+\frac{1}{t}\int_0^t\left[\int_X Z_3(x)I_{\mathrm{T}}(t^-)\tilde{N}(\mathrm{d}t,\mathrm{d}x)\right]\mathrm{d}r\\
&+\frac{1}{t}\int_0^t\left[\int_X Z_4(x)I_{\mathrm{HT}}(t^-)\tilde{N}(\mathrm{d}t,\mathrm{d}x)\right]\mathrm{d}r,\end{aligned} \tag{33}$$

where

$$\begin{aligned}M(t) ={}& \frac{\sigma_1}{t}\int_0^t S(r)\mathrm{d}W_1(r)+\frac{\sigma_2}{t}\int_0^t I_{\mathrm{H}}\mathrm{d}W_2(r)+\frac{\sigma_3}{t}\int_0^t I_{\mathrm{T}}\mathrm{d}W_3(r)+\frac{\sigma_4}{t}\int_0^t I_{\mathrm{HT}}\mathrm{d}B_4(r)\\
&+\frac{1}{t}\int_0^t\left[\int_X Z_1(x)S(t^-)\tilde{N}(\mathrm{d}t,\mathrm{d}x)\right]\mathrm{d}r+\frac{1}{t}\int_0^t\left[\int_X Z_2(x)I_{\mathrm{H}}(t^-)\tilde{N}(\mathrm{d}t,\mathrm{d}x)\right]\mathrm{d}r+\frac{1}{t}\int_0^t\left[\int_X Z_3(x)I_{\mathrm{T}}(t^-)\tilde{N}(\mathrm{d}t,\mathrm{d}x)\right]\mathrm{d}r\\
&+\frac{1}{t}\int_0^t\left[\int_X Z_4(x)I_{\mathrm{HT}}(t^-)\tilde{N}(\mathrm{d}t,\mathrm{d}x)\right]\mathrm{d}r\end{aligned}$$

is locally continuous and $M(0)=0$. Now applying Lemma 1 as $t\to\infty$, and using Eq. (24), (28), and (32), as $t\to\infty$, we have

$$\lim_{t\to\infty}\langle S(t)\rangle=\frac{\Psi}{d},\quad \text{a.s.}$$

Which prove the conclusion.

5. Persistence

In this section, we will make the examination of the long-term effects of the condition. Initially, we establish the average persistence according to the definition provided by the authors in Ref. [35].

Definition 1[35,38] We consider the persistence or preservation of system (4) under the following assumption:

$$\liminf_{t\to\infty}\frac{1}{t}\int_0^t I(r)\,\mathrm{d}r>0,\quad \text{a.s.}\tag{34}$$

We may also require fundamental results as provided by Ref. [38], to verify epidemic persistence.

Lemma 2 [(strong law)[31]] If a continuous function $\{D(t)\}_{0\le t}$ exists as a local martingale such that as $t\to 0$ it diminishes, then

$$\lim_{t\to\infty}D(t)=\infty,\quad \text{a.s.}\quad\Rightarrow\lim_{t\to\infty}\frac{D(t)}{t}=0,\quad \text{a.s.}\tag{35}$$

$$\limsup_{t\to\infty}\frac{D(t)}{t}<0,\quad \text{a.s.}\quad\Rightarrow\lim_{t\to\infty}\frac{D(t)}{t}=0,\quad \text{a.s.}\tag{36}$$

Lemma 3 Consider $j\in\mathcal{C}([0,\infty)\times\Pi,(0,\infty))$ and $J\in\mathcal{C}([0,\infty)\times\Pi,\mathbb{D})$. If

$$\lim_{t\to\infty}\frac{J(t)}{t}=0,\quad \text{a.s.}\tag{37}$$

holds for all $t\ge 0$,

$$\ln j(t)\ge\Xi_0 t-\Xi\int_0^t j(s)\,\mathrm{d}s+J(t),\quad \text{a.s.},\tag{38}$$

$$\liminf_{t\to\infty}j(t)\ge\frac{\Xi_0}{\Xi}\quad \text{a.s.},\tag{39}$$

where $\{\Xi,\Xi_0\in\mathbb{D}\mid\Xi>0\text{ and }\Xi_0\ge 0\}$.[35]

In this part, we shall outline the assumptions for the average persistence of the system (4). The fundamental objective of this section is described in the following Theorem 3.

Theorem 3 If $\mathbb{R}_0^S>1$, then for any initial approximation $(S_0,I_{\mathrm{H}0},I_{\mathrm{T}0},I_{\mathrm{HT}0},R_0)\in\mathbb{R}_+^5$, the epidemic $I_{\mathrm{H}}(t)$ satisfies the following equation:

$$\liminf_{t\to\infty}I_{\mathrm{H}}(t)\ge\frac{4\Psi\left[\sqrt{\mathbb{R}_0^{\mathrm{S}}}-1\right]}{\mathbb{C}_1(\beta_{\mathrm{H}}+\beta_{\mathrm{T}}+\beta_{\mathrm{HT}})},\quad \text{a.s.}\tag{40}$$

And similarly,

$$\liminf_{t\to\infty}I_{\mathrm{T}}(t)\ge 0,\quad \liminf_{t\to\infty}I_{\mathrm{HT}}(t)\ge 0,\tag{41}$$

where

$$\mathbb{C}_1=\frac{\delta}{\left(d+\sigma_1^2/2+\int_X[Z_1(x)-\ln(1+Z_1(x))]\nu\,\mathrm{d}x\right)}.$$

Thus, we can infer that the disease will persist in the society.

Let us state

$$\mathbb{R}_0^{\mathrm{S}}=\frac{\Psi\beta_{\mathrm{H}}\beta_{\mathrm{T}}\beta_{\mathrm{HT}}}{\left(d+\sigma_1^2/2+\int_X[Z_1(x)-\ln(1+Z_1(x))]\nu\,\mathrm{d}x\right)(b_1c_1d_1)},\tag{42}$$

where

$$b_1=\left(\alpha_1+\alpha_2+d+\frac{\sigma_2^2}{2}+\int_X[Z_2(x)-\ln(1+Z_2(x))]\nu\,\mathrm{d}x\right),$$
$$c_1=\left(\gamma_1+\gamma_2+d+\frac{\sigma_3^2}{2}+\int_X[Z_3(x)-\ln(1+Z_3(x))]\nu\,\mathrm{d}x\right),$$
$$d_1=\left(\eta_1+\eta_2+d+\frac{\sigma_4^2}{2}+\int_X[Z_4(x)-\ln(1+Z_4(x))]\nu\,\mathrm{d}x\right).$$

Proof Let,

$$y_1=-\mathbb{C}_1\ln S-\mathbb{C}_2\ln I_{\mathrm{H}}-\mathbb{C}_3\ln I_{\mathrm{T}}-\mathbb{C}_4\ln I_{\mathrm{HT}}.\tag{43}$$

In Eq. (43), $\mathbb{C}_1$, $\mathbb{C}_2$, $\mathbb{C}_3$, and $\mathbb{C}_4$ are fixed and we may calculate these later.

Utilizing Itô's formula on Eq. (43), it follows that

$$\begin{aligned}\mathrm{d}y_1=&Ly_1-\mathbb{C}_1\sigma_1\,\mathrm{d}W_1(t)-\mathbb{C}_2\sigma_2\,\mathrm{d}W_2(t)-\mathbb{C}_3\sigma_3\,\mathrm{d}W_3(t)-\mathbb{C}_4\sigma_4\,\mathrm{d}W_4(t)\\&-\mathbb{C}_1\int_X[Z_1(x)-\ln(1+Z_1(x)]\tilde{N}(\mathrm{d}t,\mathrm{d}x)-\mathbb{C}_2\int_X[Z_2(x)-\ln(1+Z_2(x)]\tilde{N}(\mathrm{d}t,\mathrm{d}x)\\&-\mathbb{C}_3\int_X[Z_3(x)-\ln(1+Z_3(x)]\tilde{N}(\mathrm{d}t,\mathrm{d}x)-\mathbb{C}_4\int_X[Z_4(x)-\ln(1+Z_4(x)]\tilde{N}(\mathrm{d}t,\mathrm{d}x),\end{aligned}\tag{44}$$

where

$$
\begin{aligned}
Ly_1 &= \mathbb{C}_1 L(-\ln S) + \mathbb{C}_2 L(-\ln I_{\mathrm{H}}) + \mathbb{C}_3 L(-\ln I_{\mathrm{T}}) + \mathbb{C}_4 L(-\ln I_{\mathrm{HT}}) \\
&= -\frac{\mathbb{C}_1\Psi}{S} + \frac{\mathbb{C}_1\beta_{\mathrm{H}} I_{\mathrm{H}}}{N} + \frac{\mathbb{C}_1\beta_{\mathrm{T}} I_{\mathrm{T}}}{N} + \frac{\mathbb{C}_1\beta_{\mathrm{HT}} I_{\mathrm{HT}}}{N} + \mathbb{C}_1 d + \frac{\mathbb{C}_1\sigma_1^2}{2} + \mathbb{C}_1\left\{\int_X \left[Z_1(x) - \ln(1+Z_1(x))\right] v\mathrm{d}x\right\} \\
&\quad -\frac{\mathbb{C}_2\beta_{\mathrm{H}} S}{N} + \frac{\mathbb{C}_2\delta_1 I_{\mathrm{T}}}{N} + \mathbb{C}_2(\alpha_1+\alpha_2+d) + \frac{\mathbb{C}_2\sigma_2^2}{2} + \mathbb{C}_2\left\{\int_X \left[Z_2(x) - \ln(1+Z_2(x))\right] v\mathrm{d}x\right\} \\
&\quad -\frac{\mathbb{C}_3\beta_{\mathrm{T}} S}{N} + \frac{\mathbb{C}_3\delta_2 I_{\mathrm{H}}}{N} + \mathbb{C}_3(\gamma_1+\gamma_2+d) + \frac{\mathbb{C}_3\sigma_3^2}{2} + \mathbb{C}_3\left\{\int_X \left[Z_3(x) - \ln(1+Z_3(x))\right] v\mathrm{d}x\right\} \\
&\quad -\frac{\mathbb{C}_4\beta_{\mathrm{HT}} S}{N} - \frac{\mathbb{C}_4\delta_1 I_{\mathrm{H}} I_{\mathrm{T}}}{N} - \frac{\mathbb{C}_4\delta_2 I_{\mathrm{T}} I_{\mathrm{H}}}{N} + \mathbb{C}_4(\eta_1+\eta_2+d) + \frac{\mathbb{C}_4\sigma_4^2}{2} + \mathbb{C}_4\left\{\int_X \left[Z_4(x) - \ln(1+Z_4(x))\right] v\mathrm{d}x\right\} \\
&\le \left(-\frac{\mathbb{C}_1\Psi}{S} - \frac{\mathbb{C}_2\beta_{\mathrm{H}} S}{N} - \frac{\mathbb{C}_3\beta_{\mathrm{T}} S}{N} - \frac{\mathbb{C}_4\beta_{\mathrm{HT}} S}{N}\right) + \mathbb{C}_1\left(d + \frac{\sigma_1^2}{2} + \int_X \left[Z_1(x) - \ln(1+Z_1(x))\right] v\mathrm{d}x\right) \\
&\quad + \mathbb{C}_2\left(\alpha_1+\alpha_2+d + \frac{\sigma_2^2}{2} + \int_X \left[Z_2(x) - \ln(1+Z_2(x))\right] v\mathrm{d}x\right) + \mathbb{C}_3\left(\gamma_1+\gamma_2+d + \frac{\sigma_3^2}{2}\right. \\
&\quad \left. + \int_X \left[Z_3(x) - \ln(1+Z_3(x))\right] v\mathrm{d}x\right) + \mathbb{C}_4\left(\eta_1+\eta_2+d + \frac{\sigma_4^2}{2} + \int_X \left[Z_4(x) - \ln(1+Z_4(x))\right] v\mathrm{d}x\right) \\
&\quad + \mathbb{C}_1\beta_{\mathrm{H}} I_{\mathrm{H}} + \mathbb{C}_1\beta_{\mathrm{T}} I_{\mathrm{T}} + \mathbb{C}_1\beta_{\mathrm{HT}} I_{\mathrm{HT}} \\
&\le -4\sqrt{\mathbb{C}_1\mathbb{C}_2\mathbb{C}_3\mathbb{C}_4\Psi\beta_{\mathrm{H}}\beta_{\mathrm{T}}\beta_{\mathrm{HT}}} + \mathbb{C}_1\left(d + \frac{\sigma_1^2}{2} + \int_X \left[Z_1(x) - \ln(1+Z_1(x))\right] v\mathrm{d}x\right) \\
&\quad + \mathbb{C}_2\left(\alpha_1+\alpha_2+d + \frac{\sigma_2^2}{2} + \int_X \left[Z_2(x) - \ln(1+Z_2(x))\right] v\mathrm{d}x\right) + \mathbb{C}_3\left(\gamma_1+\gamma_2+d + \frac{\sigma_3^2}{2}\right. \\
&\quad \left. + \int_X \left[Z_3(x) - \ln(1+Z_3(x))\right] v\mathrm{d}x\right) + \mathbb{C}_4\left(\eta_1+\eta_2+d + \frac{\sigma_4^2}{2} + \int_X \left[Z_4(x) - \ln(1+Z_4(x))\right] v\mathrm{d}x\right) \\
&\quad + \mathbb{C}_1\beta_{\mathrm{H}} I_{\mathrm{H}} + \mathbb{C}_1\beta_{\mathrm{T}} I_{\mathrm{T}} + \mathbb{C}_1\beta_{\mathrm{HT}} I_{\mathrm{HT}},
\end{aligned} \tag{45}
$$

let

$$
\begin{aligned}
\mathbb{C}_1 &= \frac{\Psi}{\left(d + \sigma_1^2/2 + \int_X \left[Z_1(x) - \ln(1+Z_1(x))\right] v\mathrm{d}x\right)}, \\
\mathbb{C}_2 &= \frac{\Psi}{\left(\alpha_1+\alpha_2+d + \sigma_2^2/2 + \int_X \left[Z_2(x) - \ln(1+Z_2(x))\right] v\mathrm{d}x\right)}, \\
\mathbb{C}_3 &= \frac{\Psi}{\left(\gamma_1+\gamma_2+d + \sigma_3^2/2 + \int_X \left[Z_3(x) - \ln(1+Z_3(x))\right] v\mathrm{d}x\right)}, \\
\mathbb{C}_4 &= \frac{\Psi}{\left(\eta_1+\eta_2+d + \sigma_4^2/2 + \int_X \left[Z_4(x) - \ln(1+Z_4(x))\right] v\mathrm{d}x\right)},
\end{aligned}
$$

let

$$
\begin{aligned}
a &= \left(d + \frac{\sigma_1^2}{2} + \int_X \left[Z_1(x) - \ln(1+Z_1(x))\right] v\mathrm{d}x\right), \\
b &= \left(\alpha_1+\alpha_2+d + \frac{\sigma_2^2}{2} + \int_X \left[Z_2(x) - \ln(1+Z_2(x))\right] v\mathrm{d}x\right), \\
c &= \left(\gamma_1+\gamma_2+d + \frac{\sigma_3^2}{2} + \int_X \left[Z_3(x) - \ln(1+Z_3(x))\right] v\mathrm{d}x\right), \\
d &= \left(\eta_1+\eta_2+d + \frac{\sigma_4^2}{2} + \int_X \left[Z_4(x) - \ln(1+Z_4(x))\right] v\mathrm{d}x\right), \\
Ly_1 &\le -4\sqrt{\frac{\Psi^4\Psi\beta_{\mathrm{H}}\beta_{\mathrm{T}}\beta_{\mathrm{HT}}}{abcd}} + 4\Psi + \mathbb{C}_1\beta_{\mathrm{H}} I_{\mathrm{H}} + \mathbb{C}_1\beta_{\mathrm{T}} I_{\mathrm{T}} + \mathbb{C}_1\beta_{\mathrm{HT}} I_{\mathrm{HT}}
\end{aligned}
$$

$$= -4\Psi\left[\sqrt{\frac{\Psi\beta_{\rm H}\beta_{\rm T}\beta_{\rm HT}}{abcd}}-1\right]+\mathbb{C}_1 I(\beta_{\rm H}+\beta_{\rm T}+\beta_{\rm HT})$$
$$= -4\Psi\left[\sqrt{\mathbb{R}_0^{\rm S}}-1\right]+\mathbb{C}_1 I(\beta_{\rm H}+\beta_{\rm T}+\beta_{\rm HT}). \tag{46}$$

By substituting Eq. (46) into Eq. (43) and integrating both sides with respect to stochastic hepatitis B problem (4), we obtain

$$\begin{aligned}\frac{y_1(S(t),I(t))-y_1(S(0),I(0))}{t} \le\ & -4\Psi\left(\sqrt{\mathbb{R}_0^{\rm S}}-1\right)+\mathbb{C}_1(\beta_{\rm H}+\beta_{\rm T}+\beta_{\rm HT})I(t)-\mathbb{C}_1\frac{\sigma_1^2W_1(t)}{t}-\mathbb{C}_2\frac{\sigma_2^2W_2(t)}{t}\\ & -\mathbb{C}_3\frac{\sigma_3^2W_3(t)}{t}-\mathbb{C}_4\frac{\sigma_4^2W_3(t)}{t}-\mathbb{C}_1\frac{\int_X[Z_1(x)S-\ln(1+Z_1(x))]\tilde{N}(\mathrm{d}t,\mathrm{d}x)}{t}\\ & -\mathbb{C}_2\frac{\int_X[Z_2(x)I_{\rm H}-\ln(1+Z_2(x))]\tilde{N}(\mathrm{d}t,\mathrm{d}x)}{t}\\ & -\mathbb{C}_3\frac{\int_X[Z_3(x)I_{\rm T}-\ln(1+Z_3(x))]\tilde{N}(\mathrm{d}t,\mathrm{d}x)}{t}\\ & -\mathbb{C}_4\frac{\int_X[Z_4(x)I_{\rm HT}-\ln(1+Z_4(x))]\tilde{N}(\mathrm{d}t,\mathrm{d}x)}{t}\\ \le\ & -4\Psi\left(\sqrt{\mathbb{R}_0^{\rm S}}-1\right)+\mathbb{C}_1(\beta_{\rm H}+\beta_{\rm T}+\beta_{\rm HT})\langle I(t)\rangle+\Pi(t),\end{aligned} \tag{47}$$

where

$$\begin{aligned}\Pi(t) =\ & -\mathbb{C}_1\frac{\sigma_1^2W_1(t)}{t}-\mathbb{C}_2\frac{\sigma_2^2W_2(t)}{t}-\mathbb{C}_3\frac{\sigma_3^2W_3(t)}{t}\\ & -\mathbb{C}_4\frac{\sigma_4^2W_2(t)}{t}-\mathbb{C}_1\frac{\int_X[Z_1(x)S-\ln(1+Z_1(x))]\tilde{N}(\mathrm{d}t,\mathrm{d}x)}{t}-\mathbb{C}_2\frac{\int_X[Z_2(x)I-\ln(1+Z_2(x))]\tilde{N}(\mathrm{d}t,\mathrm{d}x)}{t}\\ & -\mathbb{C}_3\frac{\int_X[Z_3(x)I_{\rm T}-\ln(1+Z_3(x))]\tilde{N}(\mathrm{d}t,\mathrm{d}x)}{t}-\mathbb{C}_4\frac{\int_X[Z_4(x)I_{\rm HT}-\ln(1+Z_4(x))]\tilde{N}(\mathrm{d}t,\mathrm{d}x)}{t}.\end{aligned}$$

From the strong law as stated in Lemma 2, we arrive at

$$\lim_{t\to\infty}\Pi(t)=0, \tag{48}$$

from Eq. (47), we have

$$\begin{aligned}\mathbb{C}_1(\beta_{\rm H}+\beta_{\rm T}+\beta_{\rm HT})\langle I(t)\rangle \ge\ & 4\Psi\left(\sqrt{\mathbb{R}_0^{\rm S}}-1\right)-\frac{\Pi(t)}{t}\\ & +\frac{y_1(S(t),I(t))-y_1(S(0),I(0))}{t}.\end{aligned} \tag{49}$$

Drawing from Lemma 3 and Eq. (50), the limit superior of Eq. (49) yields

$$\liminf_{t\to\infty}\langle I(t)\rangle \ge \frac{4\Psi\left(\sqrt{\mathbb{R}_0^{\rm S}}-1\right)}{\mathbb{C}_1(\beta_{\rm H}+\beta_{\rm T}+\beta_{\rm HT})}\ge 0 \quad \text{a.s.} \tag{50}$$

Thus, this implies that

$$\liminf_{t\to\infty}I_{\rm H}(t)\ge 0,\quad \liminf_{t\to\infty}I_{\rm T}(t)\ge 0,\quad \liminf_{t\to\infty}I_{\rm HT}(t)\ge 0.$$

Thus, the proof of Theorem 3 is finished.

6. Numerical scheme and simulations

To further verify the authenticity of the theoretical analysis carried out in the previous sections and to explore the inherent randomness in the underlying diseases, in this part, we give some of the numerical simulation results. The theoretical results associated with both deterministic model (1) and stochastic model (4) are numerically verified using different settings of the parameters. We choose the time interval from 0 to 200 and the initial values of the state variables as

$$(S,I_{\rm H},I_{\rm T},I_{\rm HT},R)=(150,170,150,150,70).$$

This numerical scheme will facilitate the validation of our theoretical results through simulations. Secondly, we aim to illustrate how specific variables and parameters influence the behavior of the model. By achieving these goals, our aim is to enhance our comprehension of the model's dynamics and glean insights into the impact of different factors.

For developing a numerical method tailored to model (4), we adopt a robust approach detailed in Ref. [38], which has proven effective across various studies (see Refs. [38,39]). Our

methodology assumes $x^* \in X$, $N^* \in \mathbb{N}$, $n = 0, 1, 2, \ldots, N^*$, and $\Delta t = T/N^*$ signifies the time step size over the interval $[0, T]$. Additionally,

$$N^n = S^n + I_{\mathrm{H}}^n + I_{\mathrm{T}}^n + I_{\mathrm{HT}}^n + R^n,$$
$$\Delta W_i^n = W_i(t_{n+1}) - W_i(t_n) = \sqrt{\Delta t}\,\sigma_i^n,$$

where σ_i^n are independent Gaussian random variables $\mathcal{N}$. Furthermore, ΔL^n, defined as $\Delta L^n = L(t_{n+1}) - L(t_n)$, follows a Poisson distribution with intensity ν, where $X = (0, +\infty)$ and $\nu(X) = 1$. Consequently, the numerical approach, specifically the Milstein technique applied to model (4), is structured as follows:

$$\begin{aligned}
S_{n+1} &= S_n + \left(\Psi - \frac{\beta_{\mathrm{H}} S_n I_{\mathrm{H}n}}{N} - \frac{\beta_{\mathrm{T}} S_n I_{\mathrm{T}n}}{N} - \frac{\beta_{\mathrm{HT}} S_n I_{\mathrm{HT}n}}{N} - dS_n\right)\Delta t + \sigma_1 S_n \Delta W_1^n + Z_1(x^*) S_n \Delta L_n \\
&\quad + \frac{1}{2}\sigma_1 S_n \left((\Delta W_1^n)^2 - \Delta t\right), \\
I_{\mathrm{H}(n+1)} &= I_{\mathrm{H}n} + \left(\frac{\beta_{\mathrm{H}} S_n I_{\mathrm{H}n}}{N} + \frac{\delta_1 I_{\mathrm{H}} I_{\mathrm{T}}}{N} - (\alpha_1 + \alpha_2 + d) I_{\mathrm{H}n}\right)\Delta t + \sigma_2 I_{\mathrm{H}n} \Delta W_2^n + Z_2(x^*) I_n \Delta L_n \\
&\quad + \frac{1}{2}\sigma_2 I_{\mathrm{H}n} \left((\Delta W_2^n)^2 - \Delta t\right), \\
I_{\mathrm{T}(n+1)} &= I_{\mathrm{T}n} + \left(\frac{\beta_{\mathrm{T}} S_n I_{\mathrm{T}n}}{N} - \frac{\delta_2 I_{\mathrm{T}n} I_{\mathrm{H}n}}{N} - (\gamma_1 + \gamma_2 + d) I_{\mathrm{T}n}\right)\Delta t + \sigma_3 I_{\mathrm{T}n} \Delta W_3^n + Z_3(x^*) I_{\mathrm{T}n} \Delta L_n \\
&\quad + \frac{1}{2}\sigma_3 I_{\mathrm{T}n} \left((\Delta W_3^n)^2 - \Delta t\right), \\
I_{\mathrm{HT}(n+1)} &= I_{\mathrm{HT}n} + \left(\frac{\beta_{\mathrm{HT}} I_{\mathrm{HT}n} Sn}{N} + \frac{\delta_1 I_{\mathrm{H}n} I_{\mathrm{T}n}}{N} + \frac{\delta_2 I_{\mathrm{H}n} I_{\mathrm{T}n}}{N} - (\eta_1 + \eta_2 + d) I_{\mathrm{HT}}\right)\Delta t \\
&\quad + \sigma_4 I_{\mathrm{HT}n} \Delta W_4^n + \gamma_4(x^*) I_{\mathrm{HT}n} \Delta L_n + \frac{1}{2}\sigma_4 I_{\mathrm{HT}n} \left((\Delta W_4^n)^2 - \Delta t\right), \\
R_{n+1} &= R_n + (\alpha_1 I_{\mathrm{H}n} + \gamma_1 I_{\mathrm{T}n} + \eta_1 I_{\mathrm{HT}n} - dR_n)\Delta t + \sigma_5 R_n \Delta W_5^n + Z_5(x^*) R_n \Delta L_n \\
&\quad + \frac{1}{2}\sigma_5 R_n \left((\Delta W_5^n)^2 - \Delta t\right).
\end{aligned} \tag{51}$$

Furthermore, it is important to note that, apart from the numerical technique used in this article, an alternate approach called the PPTEM method[39] may be used to achieve an approximate solution for the suggested model.

6.1. Numerical simulation on extinction

Two different discretisation approaches are used when one using computational methods to simulate stochastic processes. First, the time parameter has to be discretized. The random variables are then approximated with artificially developed finite time series datasets. To replicate a Lévy process with stable and independent increments at discrete time points, the easiest method is to generate random integers from an indefinitely divisible distribution. To explain the long-run behavior of the model and to verify the biological importance of the underlying system, we have chosen values of the parameters as $\Psi = 0.08$, $\beta_{\mathrm{T}} = 0.05$, $d = 0.02$, $\beta_{\mathrm{H}} = 0.04$, $\beta_{\mathrm{HT}} = 0.04$, $\alpha_1 = 0.20$, $\alpha_2 = 0.02$, $\eta_1 = 0.10$, $\eta_2 = 0.05$, $\gamma_1 = 0.01$, $\gamma_1 = 0.03$, $\delta_1 = 0.01$, $\delta_2 = 0.04$ and the noise intensities assumed $\sigma_1 = 0.75$, $\sigma_2 = 0.45$, $\sigma_3 = 0.35$, $\sigma_4 = 0.20$, $\sigma_5 = 0.20$, and $Z_\iota(\Upsilon) = -k_i Z(\Upsilon)/(1 + Z(\Upsilon)^2), \Upsilon = 0.5$, with $k_1 = 0.55$, $k_2 = 0.40$, $k_3 = 0.65$, $k_4 = 0.30$, and $k_5 = 0.45$.

By using these values of parameters, we estimated the threshold parameter and it was observed that $\mathbb{R}_0^{\mathrm{E}} < 1$. The necessary condition for the disease's extinction whose dynamics is given by model (4) is given in Theorem 2. The conclusion of Theorem 2 holds if and only if $\mathbb{R}_0^{\mathrm{E}} < 1$, as the numerical simulation results verify. Stochastic extinction is a notion that this behavior correctly illustrates. Since any trajectory, noise-free or with a standard distribution, behaves the same way, we refer to this situation as total extinction. Theoretically, the condition $\mathbb{R}_0^{\mathrm{E}} < 1$ ensures the existence and stability of the disease-free equilibrium point for the underlying deterministic system. Likewise, we proved results about the extinction of the disease via analyzing the stochastic model under similar conditions. We simulated the model and obtained graphical illustrations in Figs. 1(a)–1(e). If the associated threshold parameters are less than unity, the susceptible curves will always lies above the t axis as supported by Fig. 1(a). Further, the approaching of other compartments towards zero and the extinction of the disease are verified by Figs. 1(b)–1(e). By comparing the dynamics of all of the curves, we can notice that all of the curves approaching the steady state. The curves that accounts Lévy jumps have huge fluctuation but stabilizes itself very quick compare to the rest of trajectories. It is also prominent to mention that these fluctuations covers majority of the data points while fitting model (4) with data and hence

make the model more practical.

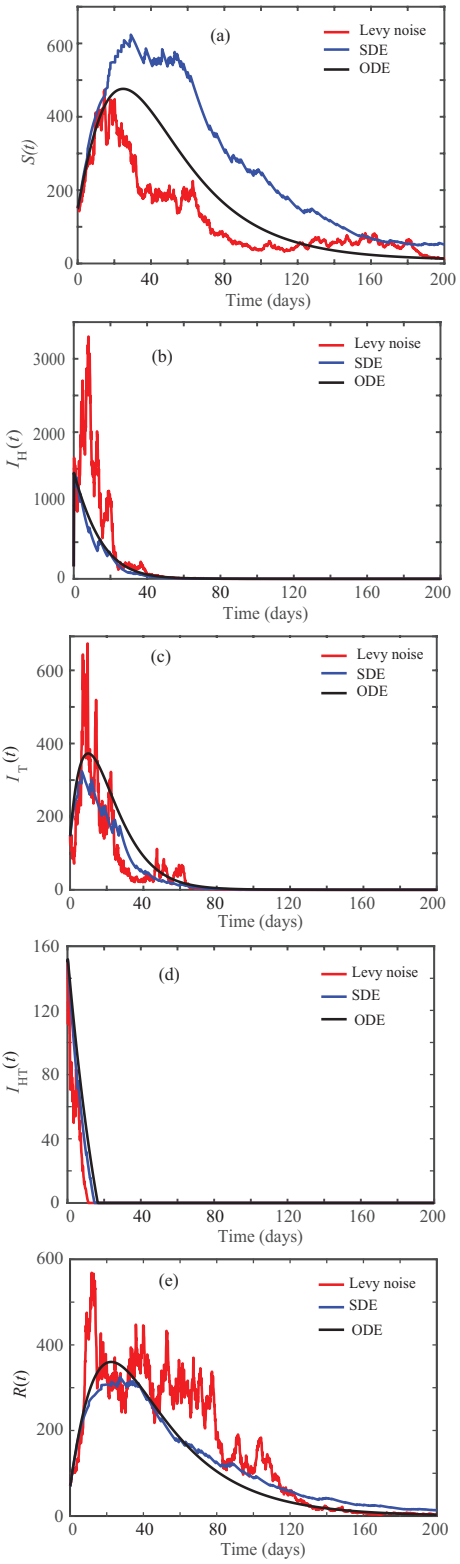


Fig. 1. The graph illustrates the dynamic behavior of the compartments $S(t)$, $I_{\rm H}(t)$, $I_{\rm T}(t)$, $I_{\rm HT}(t)$, and $R(t)$, comparing the results from the stochastic system (SDE with Lévy and white noises) to those from the underlying deterministic system. This behavior is observed when the corresponding threshold parameters are below unity, highlighting the long-run dynamics of the respective population. (a) The dynamic behavior of the class $S(t)$ when the respective thresholds are less than one, (b) the plot illustrates the behavior of the $I_{\rm H}$ compartment over time, (c) the graph depicts the long-term behavior of $I_{\rm T}(t)$ class as time progresses, (d) the dynamics of $I_{\rm HT}$-compartment over time under the condition $\mathbb{R}_0^E < 1$, (e) the plot illustrates the change in the $R(t)$ compartment over time.

6.2. Numerical simulation on persistence

Let us now explore the scenario of the persistent infection. We verify the persistence of the disease in numerically and we take the parameter values as follows: $\Psi = 0.80$, $\beta_{\rm T} = 0.58$, $d = 0.50$, $\beta_{\rm H} = 0.40$, $\beta_{\rm HT} = 0.50$, $\alpha_1 = 0.20$, $\alpha_2 = 0.20$, $\eta_1 = 0.10$, $\eta_2 = 0.05$, $\gamma_1 = 0.10$, $\gamma_1 = 0.20$, $\delta_1 = 0.30$, $\delta_2 = 0.40$, and the noise intensities assumed to be $\sigma_1 = 0.55$, $\sigma_2 = 0.70$, $\sigma_3 = 0.30$, $\sigma_4 = 0.50$, $\sigma_5 = 0.40$, and $Z_i(\Upsilon) = -k_i Z(\Upsilon)/(1+Z(\Upsilon)^2)$, $\Upsilon = 0.5$, with $k_1 = 0.55$, $k_2 = 0.35$, $k_3 = 0.70$, $k_4 = 0.30$, and $k_5 = 0.45$. By using these values of parameters, we estimated the threshold parameter and observed that $\mathbb{R}_0^S > 1$, indicating that the hypothesis of the Theorem 3 are fulfilled. This suggests that even under the influence of a weak noise, the epidemic will persist rather than dying out.

The numerical simulations confirm this conclusion, as shown in Figs. 2(a)–2(e), where the epidemic curves obtained from system (4) remains stable around the average disease value. This behavior of model's trajectories supports the conclusions of the Theorem 3. It could be noticed from the figures that over an extended period, the intensity of the noise affects the extent to which the solution fluctuates around the deterministic equilibrium states. In particular, the temporal average tends to align closely with the endemic equilibrium, especially at lower noise intensities. This finding underscores the importance of considering environmental fluctuations in biological dynamics.

Moreover, the stochastic volatility sometimes exhibits significant upward jumps and clusters at high levels, further emphasizing the impact of the noise. In contrast to the scenario where $\mathbb{R}_0^E < 1$ and the necessary condition for disease extinction is met (as discussed in Theorem 2), the case of $\mathbb{R}_0^S > 1$ shows that the epidemic persists, even under the weak noise. This persistence is in the stark contrast to the concept of the stochastic extinction, where trajectories behave the same way regardless of the noise, leading to the total extinction. Here, the persistence and fluctuations highlights the model's adaptability to real-world scenarios, making the model more practical and realistic. The trajectories with Lévy jumps are visible with huge fluctuations particularly as shown in Figs. 2(b) and 2(e). Due to its quality of covering more data points, the amplitude of fluctuations of the curves accumulating Lévy jumps around the deterministic equilibrium states are much higher in comparison with the SDE. Like in the case of the extinction, here too, the curves with Lévy jumps quickly stabilizes itself appealing the utilization of Lévy jumps in the stochastic modeling.

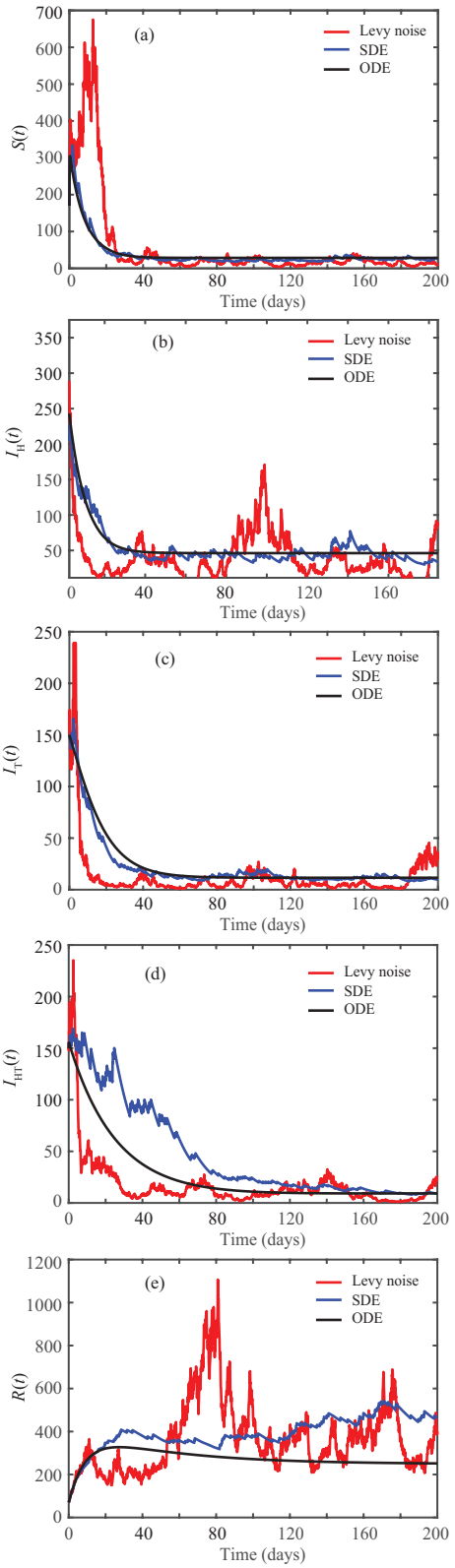


Fig. 2. The graph compare the outcomes of the underlying deterministic system with the stochastic system (4) (SDE with both Lévy and white noise), explaining the dynamic behavior of the compartments $S(t)$, $I_{\mathrm{H}}(t)$, $I_{\mathrm{T}}(t)$, $I_{\mathrm{HT}}(t)$, and $R(t)$. The results are based on persistence of the disease assuming that the associated threshold parameters are greater than one. (a) The change in $S(t)$-compartment when the respective thresholds exceeds unity, (b) the dynamic behavior of the class $I_{\mathrm{H}}(t)$ explaining persistence of the disease, (c) he graph depicts the long-term behavior of $I_{\mathrm{T}}(t)$-class as time evolves when the values of the thresholds are greater than one, (d) the dynamics of I_{HT}-compartment over time under the condition $\mathbb{R}_0^{\mathrm{D}}$ and $\mathbb{R}_0^{\mathrm{E}}$ are greater than unity, (e) the plot illustrates the change in the $R(t)$ compartment over time.

6.3. Impact of parameters β_{H}, β_{T}, and β_{HT}

In this part of the manuscript, we will explore the relative impact of the parameters $\beta_{\mathrm{H}}, \beta_{\mathrm{T}}, \beta_{\mathrm{HT}}$ on the dynamic behavior of the classes I_{H}, I_{T}, and I_{HT} obtained from model (4). The rest of the parameters have been fixed and assumed from the section describing the extinction of the disease. Figure 3(a) shows the overall progress in the compartment I_{H} while considering three different values of β_{H}. The figure suggests a direct relation between the variable and parameter. We can notice that with an increase in β_{H}, the corresponding infection tends to grow and further, the fluctuation of the stochastic curve tend to increase. Figure 3(b) explains the dynamics of the I_{T}-class keeping in view three different values of β_{T}. The figure suggests that infection due TB will continue to grow as we increase the corresponding transmission coefficient. Further, the fluctuation in the I_{T} curves tend to increase with an increase in β_{T}. A similar relationship could be built in state variable I_{HT} and β_{HT} as explained in Fig. 3(c).

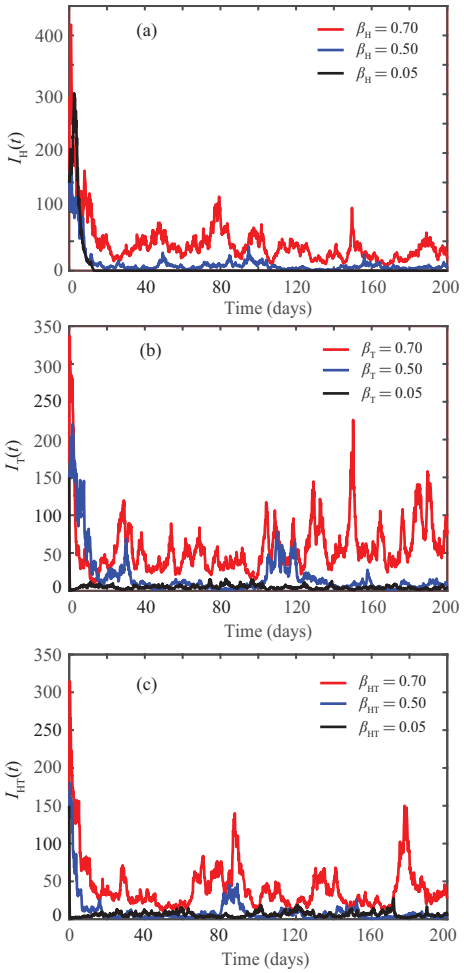


Fig. 3. The relative impact of the parameters β_{H}, β_{T}, β_{HT} on the infected compartments obtained from system (4). (a) The plot shows the relative impact of the parameter β_{H} on the state variable $I_{\mathrm{H}}(t)$, (b) the plot depicts the impact of the parameter β_{T} on the TB infection, (c) the graph explains how the compartment $I_{\mathrm{HT}}(t)$ behaves as a variation occurs in values of the parameter β_{HT}.

By analyzing all subplots in Fig. 3, we can see that the influence on the class infected compartment tends to diminish with decreasing values of β_{H}, β_{T}, β_{HT}. Thus, the parameters β_{H}, β_{T}, β_{HT} and the infection variables are directly related. For stochastic curves, it seems sense that the relationship would appear to be inverse. The primary explanation for this is that infection intensities are a major factor in whether the virus spreads among people or not. Therefore, if one were to lower the β_{H}, β_{T}, β_{HT} values, co-infection might be avoided and managed. By reducing the transmission coefficient and assuming sufficiently high stochastic disturbances, it is possible to completely eradicate co-infection. The overall picture of this simulation is that for reducing all three types of infection, one must decrease values of the underlying parameters called the transmission coefficients.

6.4. Impact of Lévy noise

As stated in the above subsections, the impact of the Lévy noise on the dynamic behavior of a stochastic model is not ignorable. Therefor, in this section, we simulated model (4) and impact of both noises on the dynamics of the model as described in Figs. 4(a) and 4(b).

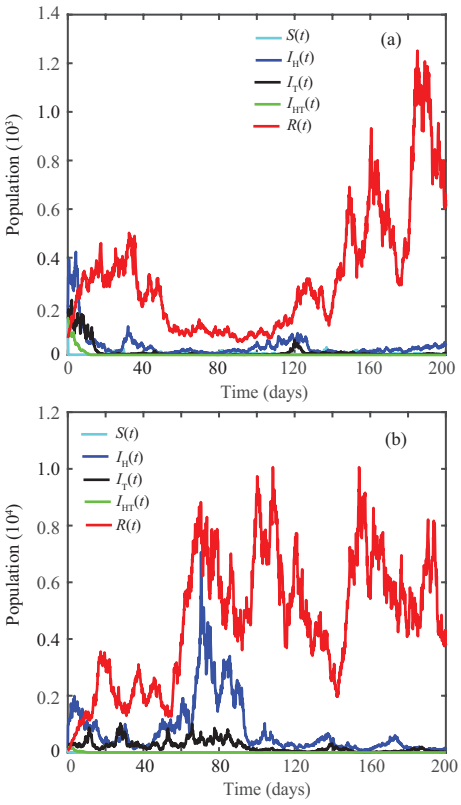


Fig. 4. The random system (4) describes the behavior of the impact of noise. (a) When $\sigma_1 = 0.75$, $\sigma_2 = 0.60$, $\sigma_3 = 0.80$, $\sigma_4 = 0.55$, $\sigma_5 = 0.45$, (b) when $\sigma_1 = 0.70$, $\sigma_2 = 0.40$, $\sigma_3 = 0.70$, $\sigma_4 = 0.50$, $\sigma_5 = 0.40$.

For both single and co-infected compartments, it is shown that increasing noise intensities accelerates the process of extinction. This simulation confirms that the solutions of the stochastic system oscillate around the endemic equilibrium for modest noise intensities, which is consistent with the findings of Theorem 3. The solution does not, however, oscillate about the EEP for bigger values of the white noise terms. This demonstrates that persistent attempts to increase stochastic disruptions via vulnerable people, together with providing appropriate care and treatment for those who are sick, might significantly lessen the transmission and circulation of co-infection within the community as depicted in Fig. 4. Moreover, the fluctuations in the curves with Lévy noises are higher while keeping the intensities at lower values.

7. Discussion

This study introduced a novel stochastic model to understand the co-infection dynamics of hepatitis B and tuberculosis. The model was investigated for a global positive solution using the Lyapunov functional theory. The model was further checked for extinction and persistence properties and it was proved that when $\mathbb{R}_0^S < 1$, both of the diseases tend to extent. For $\mathbb{R}_0^S > 1$, the co-infection exist and in such scenario, the stochastic curves oscillate around the endemic equilibrium of the deterministic model. Both the extinction and persistence of the infections were confirmed through simulations. A convergence toward the steady state may be shown in the extinction situation by comparing the dynamics across all curves. The Lévy jump curves, in particular, show notable oscillations but stabilize faster than the others as shown in Fig. 1. The model is more reliable and useful in real-world situations since these variations span various data points. This shows that to more accurately represent the intricate dynamics seen in real biological systems, stochastic components like Lévy leaps must be included. These results, taken together, support the model's applicability in forecasting disease behavior and guiding successful management measures. Figure 2 intends to portray the case of persistence. From the figure, it is evident that noise intensity has a long-term effect on how much the solution oscillates about the deterministic equilibrium states. Interestingly, the temporal average generally agrees well with the endemic equilibrium, especially at lower noise levels. This emphasizes how important oscillations in the environment are to biological processes. Furthermore, stochastic volatility periodically exhibits notable upward leaps and clusters at high levels to highlight the effect of noise. Here, the model's adaptation to actual events is highlighted by its persistence and fluctuations, which add to its practicality and realism. There are noticeable variations in the trajectories that have Lévy leaps. Curves with Lévy leap around the deterministic equilibrium because of their increased capacity to encompass a greater number of data points.

We also numerically investigated the impact of parameters β_{H}, β_{T}, β_{HT} on the infection variables. Referred to Fig. 3, we obtained that these parameters and variables are strongly correlated. Naturally, the connection should appear to be inverse for stochastic curves. The main theory explaining this is that viral transmission between individuals is largely dependent on the severity of the infection. As a result, co-infection may be prevented and controlled if the values of β_{H}, β_{T}, β_{HT} decline. Complete elimination of co-infection is achievable if the transmission coefficient is decreased and strong enough stochastic disturbances are assumed. In this simulation, the general result is that lower values of the underlying parameters, known as the transmission coefficients, are required to reduce all three forms of infection. It is crucial to note that there are some reasons why the proposed model and observations are not entirely perfect. The findings are based on both local mathematical analysis and a model that ignores many common aspects, including the influence of human behavior, various other structuring variables, and the growth of antibiotic-resistant to tuberculosis. Since this is the first time the dynamics of HBV–TB co-infection have been examined, a research program addressing these determinants is still necessary.

8. Conclusion remarks

In this study, we have introduced a novel stochastic model for exploring the co-infection dynamics of TB and hepatitis B. It was demonstrated that a positive global solution to the stochastic model exists and is unique. The case in which the solution of the proposed system oscillating around the deterministic model's endemic equilibrium is determined by formulating the Lyapunov function. Furthermore, the co-infection model was investigated for the persistence and suitable conditions were derived. To verify theoretical findings on the extinction and durability of co-infection between tuberculosis and TB in the community, numerical simulations were conducted. We studied the cases when the related threshold numbers, both stochastic and deterministic, are more than one and below one. Subsequently, we confirmed the derived theoretical results through simulations for different scenarios of the threshold parameter. Biologically, both the extinction and persistence of the infections were confirmed through simulations. Additionally, graphical illustrations are provided explaining the random fluctuations brought on by stochastic Lévy noises. A convergence toward the steady state may be shown in the extinction situation by comparing the dynamics across all curves. The Lévy jump curves, in particular, show notable oscillations but stabilize faster than the others. According to numerical data and already conducted research on the co-dynamics of these infections, increasing funding to lower HBV prevalence may be a useful strategy for limiting or controlling the effects of tuberculosis. Programs that expedite the treatment of active TB patients, however, may result in notable decreases. Given that there are around 8 million new cases of active tuberculosis each year, a program could be possible. Insights into disease interactions and a basis for future research exploring more complicated interactions and additional elements for wider applications are provided by this study, which tackles important aspects of the dynamics of co-infection between tuberculosis and herpesvirus.

The future research could focus on incorporating additional factors such as multi-drug resistance, varying transmission rates in different populations, and the impact of vaccination programs. Additionally, exploring co-infections with other diseases, socio-economic factors, and the effect of public health interventions on long-term dynamics could provide more comprehensive insights. One can also think about age-structure, delay effect and non-Gaussian noise in such and related studies in future.

References

[1] World Health Organization 2019 *Global Tuberculosis Report* Retrieved from WHO
[2] World Health Organization 2017 *Global Hepatitis Report* Retrieved from WHO 2017
[3] Onyebujoh P, Thirumala A K and Ndihokubwayo J B 2016 *African Journal of Laboratory Medicine* **5**
[4] Guo B Z and Cai L M 2011 *Mathematical Biosciences and Engineering* **3** 689
[5] Alkhazzan A, Wang J, Nie, Y, Khan H and Alzabut J 2024 *Math. Meth. Appl. Sci.* 1
[6] Alkhazzan A, Wang J, Nie Y, Khan H and Alzabut J 2023 *Chaos, Solitons and Fractals* **175** 113953
[7] Din A 2021 *Chaos* **31** 12
[8] Hosaka T, Suzuki F, Fujiyama S, Kawamura Y and Sezaki 2022 *Hepatology Communications* **6** 36
[9] Khan T, Faiz M and Khan Z U 2024 *Mathematical Techniques in Modeling* **1** 11
[10] Khan W A, Zarin A, Zeb A, Khan Y and Khan A 2024 *Mathematical Techniques in Modeling* **1** 25
[11] Jiao Y, Chunhua Z and Yuhui L 2023 *Chaos* **9** 1
[12] Din A, Yongjin L and Shah M A 2021 *Journal of Systems Science and Complexity* **34** 1301
[13] Ain Q 2021 *Journal of Mathematical Techniques in Modeling* **1** 52
[14] Shah A, Tahir H, Khan A and Arshad A 2024 *Journal of Mathematical Techniques in Modeling* **1** 75
[15] Din A, Khan A and Dumitru B 2020 *Chaos, Solitons and Fractals* **139** 110036
[16] Benedetto E 2021 Reply to the Comment on "On the general relativistic framework of the Sagnac effect" [Eur. Phys. J. Plus (2020) **135** 234] *The European Physical Journal Plus 20* 111
[17] Luo Y, Zeng C and Li B 2022 *Europhys. Lett.* **2** 21002
[18] Luo Y, Zeng C and Ai B 2022 *Phys. Rev. E* **4** 042114
[19] Alkhazzan A, Wang J, Nie Y, Khan H and Alzabut J 2024 *Chaos, Solitons and Fractals* **181** 114631
[20] Feng F, Jiaqin W, Qingjia C, Shunshun W, Wanqian L, Li Y, Guanbin S, Lianhong P, Kang X and Chunli W 2024 *Adv. Sci.* 2405975
[21] Duan X, Dongsheng X, Runtian Z, Xiaotian L, Jiali S, Chao Q, Xinya S and Changsheng L 2023 *Cyborg and Bionic Systems* **4** 0013
[22] Ji C, Jiang D and Shi N 2012 *Anal. Appl.* **30** 755
[23] Ru L, Song Y and Jiang G P 2021 *Chin. Phys. B* **30** 120202
[24] Hyman M and Ann E Stanley 1988 *Mathematical Biosciences* **90** 415

[25] Din A, Amine S and Allali A 2023 *Nonlinear Dyn.* **111** 1921
[26] Andrew O, Abbas M and Din A 2023 *Mathematics and Computers in Simulation* **204** 302
[27] Naresh R and Tripathi A 2005 *Anal.* **10** 275
[28] Bacaer N, Ouifki R, Pretorious C, Wood R and William B 2008 *Math. Biol.* **57** 557
[29] Sharomi O, Podder C, Gumel A and Song B 2008 *Math. Biosci. Eng.* **5** 145
[30] Roeger L, Feng Z and Chavez C 2009 *Math. Biosci. Eng.* **6** 815
[31] Mao X 1997 *Stochastic differential equations and their applications* (Chichester: Horwood)
[32] Din A and Li Y J 2022 *Chin. Phys. B* **31** 020202
[33] Zhao Y and Jiang D 2014 *Appl. Math. Comput.* **243** 718
[34] Luo Y, Zeng C, Huang T and Ai B Q 2022 *Phys. Rev. E* **3** 034208
[35] Murad A, Nie Y, Din A and Alkhazzan 2024 *Mathematics* **12** 1645
[36] He L F, Cui Y Y, Zhang T Q, Zhang G and Song Y 2016 *Chin. Phys. B* **25** 060501
[37] Bowong S and Kurths 2010 *Mathematical Modelling of Natural Phenomena* **6** 96
[38] Danane J, Allali K, Hammouch Z and Nisar K 2021 *Results in Physics* **23** 103994
[39] Mao X, Wei F and Wiriyakraikul T 2021 *Comput. Appl. Math.* **394** 113566